VALIDATION OF AIRS/AMSU/HSB CORE PRODUCTS *for* Data Release Version 3.0

Edited by:
E. Fetzer

Contributions by:

H. H. Aumann, Frederick Chen, Luke Chen, Steve Gaiser, Denise Hagan, Thomas Hearty, Frederick W. Irion, Sung-Yung Lee Larry McMillin, Edward Olsen, Hank Revercomb, Phil Rosenkranz, David Staelin, Larrabee Strow, Joel Susskind, David Tobin, and Jiang

Version 1.0 **August 13, 2003**
JPL D-26538

ABSTRACT

This report describes validation comparisons for AIRS, AMSU and HSB data products. A more detailed synopsis is given in the Executive Summary section, and individual chapters describe the analyses in detail.

Comparisons are limited to observed radiances, retrieved sea surface temperature (SST), and retrieved temperature and humidity profiles. Preliminary analyses for ozone are presented in an appendix. The results for both observed radiances and retrieved products apply to oceans for latitudes from 40S to 40N. Retrieved product validation results apply only to those situations where a full infrared retrieval was completed, or about 70% of over-water retrieval footprints. Retrieval results are further limited to those retrievals whose SST agree with Real Time Global SST to within ±3 K, affecting about 7% of total retrievals.

AIRS observed infrared radiances are compared with aircraft observations, and with radiances calculated from European Center for Mediumrange Weather Forecasting (ECMWF) assimilation model analyses and radiosondes. These show AIRS to be operating as characterized by pre-launch calibration measurements. Frequency-dependent AIRS radiance uncertainties are between about 0.1 and 0.5 K in brightness temperatures, with biases typically much less than 0.1 K. The infrared forward model uncertainties are roughly 0.5 K for those spectral regions originating at the surface or in the lower troposphere; data limitations prevent complete spectral comparisons above about 500 mb for water vapor. AMSU and HSB observed radiances are affected by sidelobes that contribute scan angle-dependent biases of 0.67 to 1.0 K, characterized through comparisons with radiosondes and with AMSU on NOAA-16. Standard deviations for the microwave instruments are 2.2 K or less. The AIRS Vis/NIR radiance uncertainties are 7 to 11% compared against a well-instrumented ground site.

Maps of retrieval pre-screening locations using a 3 K SST threshold are consistent with regions of sun glint, stratus and cirrus clouds, dust, scene inhomogeneities, and cloud formations that may cause retrieval degeneracies. All of these phenomena degrade retrieval quality.

Differences in retrieved cloud cleared radiances with those calculated from ECMWF vary from about 0.5 K to 3 K, depending on cloud amount.

Retrieved SST are compared against ECMWF, with differences of -0.8 K ± 1.0 K. Differences against buoys are -0.8 K ± 1.1 K. Both results are skewed by rejection of retrievals deviating from forecast by more than 3 K. SST comparisons with a ship-borne radiometer are -0.85 ± 1.2 K.

Retrieved temperature profiles are compared with ECMWF, and with dedicated radiosondes. Root-mean-square temperature differences against ECMWF vary from about 1.3 K just above the surface to less than 1 K in the troposphere when averaged over 1 km thick layers, with biases of 0.2 K or less. Dedicated radiosondes give uncertainties of less about 1 K in retrieved temperature in the free troposphere.

Retrieved total water vapor compared against ECMWF, and operational and dedicated sondes agrees to within 11 to 16% rms. Total water vapor biases are generally 3% or less, but about 10% at Nauru, located in a region of very large water vapor loading in the equatorial western Pacific. Retrieved water vapor profiles are compared with

ECMWF and operational sondes. Biases with sondes are –3.7 to 3.6% up to 300 mb; biases against the model are also small below 500 mb, but increase to –13% or more above 500 mb.

Root-mean-squared differences between water vapor retrievals and other observations increase with height from 10-14% near the surface to 33-50% above 500 mb.

AIRS total column ozone differs from TOMS globally by 4.4 ± 5.3%.

Table of Contents

Tables

Figures

1. Introduction

1.1. Overview

This report describes the validation of AIRS/AMSU/HSB products. Validation is the comparison between those products and other data describing the atmosphere. Those other data come from a variety of sources described briefly in Section 1.5 below, and in more detail in later sections. Retrieved products are validated for the following sets of conditions:

- *Low latitudes only* (40 South to 40 North).
- *Ocean* (land fractions less than 0.01)
- *Agreement with NCEP analyses to with 3.0 K*

The Aqua spacecraft was launched on 5 May 2002. The AMSU and HSB instruments were operational within one week of launch. The AIRS instrument has been in operation almost continuously since 30 August 2002. During operations the instruments observe collocated microwave, infrared and near-infrared measurements. These result in about 324,000 sets of radiance observations and associated retrievals per day. Each set of radiance observations yields retrieved quantities including cloud properties and surface temperatures, plus profiles of temperature and humidity. This report describes their validation over oceans between 40 S and 40 N. An overview of the validation status of the AIRS data sets is given in the Executive Summary in Section 2 below.

HSB ceased operating on 5 February 2003, despite several attempts to restart it. *This report addresses primarily the first six months of AIRS / AMSU / HSB operations, when HSB was fully functional.* Assessing the impact of the loss of HSB is an ongoing activity for the AIRS project.

1.2. Validation Status: Beta and Provisional

This report addresses the validation of AIRS / AMSU / HSB Core Products, as shown in Table 1 below. While all AIRS / AMSU / HSB data are released in v3.0, only observed radiances are provisionally validated. The terms provisional, beta and validated are defined below (See AIRS QA Plan, 2002, listed below in Supporting Documents in Section 1.4).

Beta -- Early release product, minimally validated and may still contain significant errors. Available to allow users to gain familiarity with data formats and parameters but not appropriate as the basis for quantitative scientific publications. *Beta validated products in the Version 3.0 data release include microwave radiances and retrieved temperature and humidity fields.*

Provisional -- Product quality may not be optimal and incremental product improvements are still occurring. General research community is encouraged to participate in the QA and validation of the product, but need to be aware that product validation and QA are ongoing. Users are urged to contact science team

representatives prior to use of the data in publications. Provisional products may be replaced in the archive when the validated product becomes available. *Provisionally validated products in the Version 3.0 data release include AIRS infrared and Visible / Near Infrared radiances.*

Validated -- Formally validated product, although validation is still ongoing. Uncertainties are well defined, and products are ready for use in scientific publications, and by other agencies. There may be later improved versions of these products. *No AIRS/AMSU/HSB products are fully validated as part of the Version 3.0 data release.*

Many aspects of the operations of these instruments are described in the *IEEE Transaction on Geosciences and Remote Sensing* Aqua special issue, Volume 41, Number 2. This report assumes the reader is familiar with this publication, and it will be referenced many times below (See References at end of this document). Other supporting documents are listed in Section 1.4 below.

.

	Version	3.0	4.0	5.0	6.0	7.0	8.0
	Activation Date	7/1/03	9/17/04	6/24/05	3/24/06	12/15/06	9/21/07
Radiance Products (L1)							
	AIRS Radiance	***Prov***	Val2	Val4	Val5		
	VIS/NIR Radiance	***Prov***	Val2	Val4	Val5		
	AMSU Radiance	***Beta***	Prov	Val2	Val4	Val5	
	HSB Radiance	***Beta***	Prov	Val2	Val4	Val5	
Standard Products (L2)							
	Cloud-Clear IR Radiance	***Beta***	Val2	Val3	Val4	Val5	
	Surface Temperature	***Beta***	Val2	Val3	Val4	Val6	
	Temperature Profile	***Prov***	Val2	Val3	Val4	Val5	
	Humidity Products	***Beta***	Val1	Val2	Val3	Val4	Val5
	Cloud Cover Products	***N/A***	Beta	Val1	Val2	Val2	Val3

Beta = Not suitable for scientific investigations. Consult with AIRS Project on regional status.
Prov = Provisionally validated. Useable for scientific investigations with caution. Validated for nonpolar night ocean only
Val1 = non-polar day/night ocean. Val2 = Val1 + non-polar night land. Val3 = Val2 + nonpolar day land Val4 = Val3 + polar night Val 5= Val 4 + polar day. Only Val5 data are useable for truly global scientific investigations.

Table 1. AIRS /AMSU/HSB data products and schedule of their validation status. Version 3.0 products are shaded. Non-polar in the version 3.0 release means latitudes between 40 S and 40 N.

1.3. Data Processing

The AIRS Science Processing System is a collection of programs, or Product Generation Executables (PGEs), used to process AIRS Science Data. These PGEs process raw, low level AIRS Infrared, AIRS Visible, AMSU, and HSB instrument data to obtain radiances, and, geophysical quantities such as temperature and humidity profiles. AIRS PGEs can be grouped into three distinct processing phases. The first phase generates instrument counts (Level 1A products) from instrument packets telemetered from the Aqua spacecraft. The second processing phase generates calibrated radiances (Level 1B products) from Level 1A. The third processing phase generates geophysical quantities (Level 2 products) from Level 1B via the retrieval algorithms. This report addresses only Level 1B and Level 2 products since Level 1A products are not geophysically meaningful and are not publicly available. The AIRS / AMSU / HSB standard data processing is shown schematically in Figure 1.

In addition to the standard processing PGEs, Browse PGEs produce aggregate summaries for standard products in Level 1B and Level 2. The Browse products are not addressed in this report as they are intended as qualitative summaries of the radiance and geophysical products.

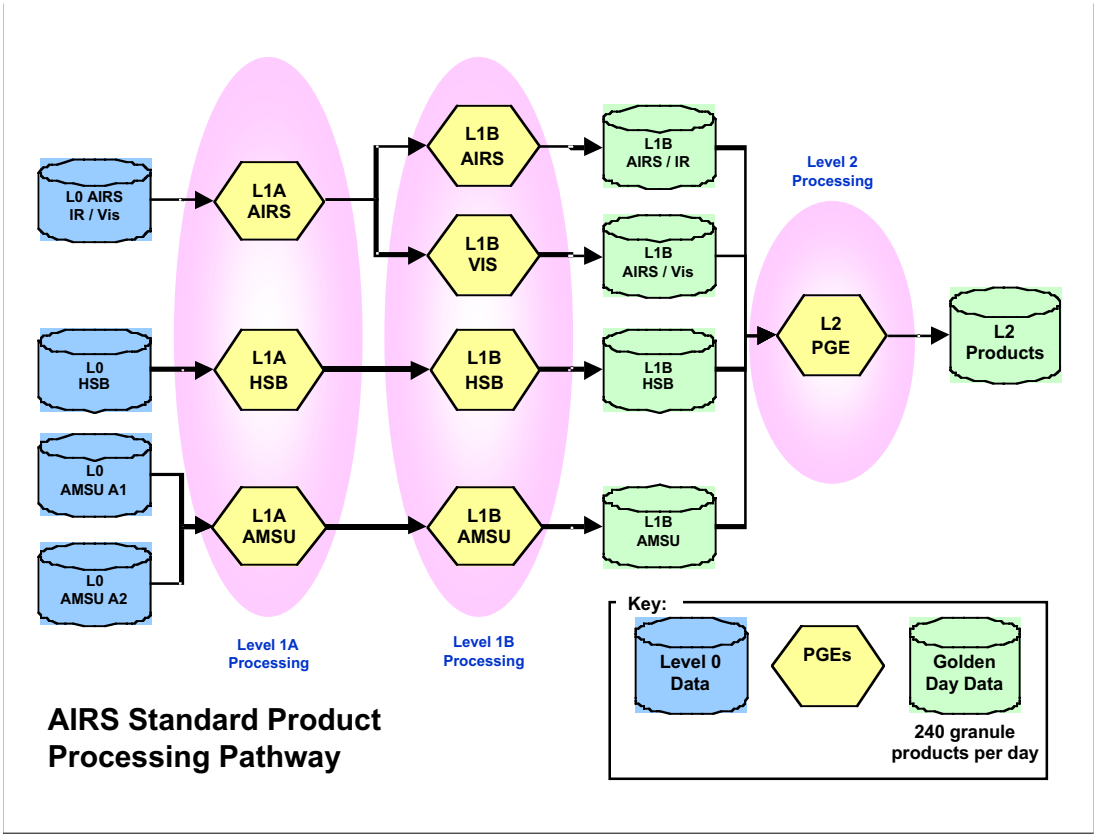

Figure 1. AIRS / AMSU / HSB data processing stages.

1.4. Supporting Documents

The following documents provide important supporting material to this Plan. See also the References at the end of this document. The AIRS Validation Plan is:

The AIRS Team Science Data Validation Plan, Version 2.1.1, JPL D-16822, June 2000.

Reports by the AIRS Validation Team are available under links to individual investigators at http://eospso.gsfc.nasa.gov/validation/pmval.php.

An overview of the AIRS instrument, and measurement requirements are given in:

AIRS Science and Measurement Requirements Document, JPL D-6665 Rev 1 September 1991 AIRS Brochure.

The AIRS calibration activities are detailed in:

AIRS Instrument Calibration Plan, JPL D-16821, Preliminary, October 14, 1997

The Algorithm Theoretical Basis Documents describe detailed operations of the processing algorithms. They are:

AIRS Algorithm Theoretical Basis Document, Level 1B, Part 1: Infrared Spectrometer, JPL D-17003, Version 2.2i, November 10, 2000

AIRS Algorithm Theoretical Basis Document, Level 1B, Part 2: Visible/Near-Infrared Channels JPL D-17004, Version 2.2, November 10, 2000

AIRS Algorithm Theoretical Basis Document, Level 1B, Part 3: Microwave Instruments, Version 2.1, JPL D-17005, Version 1.2, November 10, 2000

AIRS Algorithm Theoretical Basis Document, AIRS-Team Unified Retrieval For Core Products, Level 2, JPL D-17006, Version 2.2, April 26, 2001

See also:

AIRS / AMSU / HSB Data Processing and Data Products Quality Assessment Plan, Version 1.0, JPL D-20748, April 3, 2002.

Atmospheric Infrared Sounder (AIRS) Level 1B Visible, Infrared and Telemetry Algorithms and Quality Assessment (QA) Processing Requirements, Version 1.0, JPL D-20046, ADF-525, June 22, 2001.

AIRS Visible and Infrared In-Flight Calibration Plan, version 2.0, JPL D-18816, ADFM 412A, May 2001.

AIRS Level 1B Visible, Infrared and Telemetry Algorithms and Quality Assessing Processing Requirements, version 1.0, JPL D-20046, ADFM 525, June 2001.

Interface Control Document Between EOSDIS Core System (ECS) and Science Computing Facilities, Revision C, December 1999. ECS Document 505-41-33.

Revision to AIRS Calibration PSAs, ADFM 537, August 20, 2001.

AIRS Version 2.1 Processing Files Description version 5.0, January 2001. JPL D-20001.

1.5. Validation Data Sets Utilized

The analyses in this report describe comparison with data sets from several sources. These include:

- *ECMWF and NCEP Analyses*. AIRS / AMSU / HSB radiances and retrieved products are compared with assimilation analyses from the European Center for Mediumrange Weather Forecasting (ECMWF) and National Center for Environmental Prediction (NCEP). Radiance comparisons utilize radiances calculated from the analysis model geophysical state, while retrieved quantities are directly compared with like fields in the analyses. Model analysis comparisons have the advantage of global coverage and known uncertainties. The former property is particularly useful for the Version 3.0 data release, restricted to ocean regions between 40 S and 40 N, because these areas have limited coverage by operational radiosondes.
- *Operational Buoys*. Operational buoy observations of sea surface temperature (SST) permit two types of validation analyses. First is a radiance comparison for modeled upwelling radiances, particularly in window channels little affected by the intervening atmosphere. The second type of comparison is with retrieved SST.
- *Operational Radiosondes*. Operational radiosondes have the advantage of large numbers, but the disadvantage of being limited primarily to northern continental regions. Fortunately, the Aqua spacecraft local time overpass time of 1:30 AM and PM places it over data-rich Europe with two hours of the 0 UTC and 12 UTC sonde launch times.
- *AIRS-dedicated Radiosondes.* Radiosondes have been launched from a number of sites around the globe during Aqua overpasses. Dedicated radiosondes have the advantage of minimal mismatch errors caused by local trends or gradients in the atmosphere. Also, some launch sites are oceanic, so are particularly relevant to the Version 3.0 data release.
- *Experiments of Opportunity These* include aircraft underflights and a campaign to validate AIRS Visible / Near Infrared observations.
- *Other AIRS-dedicated Observations* The field experiments supporting AIRS validation are described at http://eospso.gsfc.nasa.gov/validation/pmval.php

2. Executive Summary

The following summarizes the results of each section. Details of those analyses are given in each section.

- Chapter 3. *Calibration, Forward Model and Computational Errors*. Infrared calibration errors vary strongly with wavelength, but are often less than 0.1 K in brightness temperature, and usually less than 0.5 K. Infrared forward model errors are less than 1 K, and generally less than 0.5 K, though information about upper tropospheric water vapor is insufficient to constrain the associated uncertainties. Computational errors in the retrievals are roughly 0.5 K in temperature, and between about 5 and 15 % for water vapor. See sections 5.1 and 5.2 for discussion of microwave calibration errors determined post launch.
- Chapter 4. *Case Study*. Radiances and retrieved quantities are compared with in situ observations for a case known to be clear. Results are within system specifications.
- Section 5.1. *Beta Validation of Advanced Microwave Sounder Observed Radiances*. Comparison with radiances calculated from dedicated and operational sondes shows AMSU standard deviations vary between about 0.3 and 0.8 K, and biases vary between about 0.6 and 3.5 K, with strong scan angle dependence. These biases are due to sidelobe contamination, and will be corrected in later data releases.
- Section 5.2. *Beta Validation of Humidity Sounder for Brazil Observed Radiances.* The HSB instrument ceased operation on 5 February 2003, and has not been restarted. Comparison with radiances calculated from dedicated and operational sondes shows HSB standard deviations range from 1 to 2.2 K, while biases range from –0.27 to 0.90 K. Similar results were obtained by comparing with AMSU on NOAA-16. HSB will need less sidelobe correction than AMSU.
- Section 5.3.1. *Stability of AIRS Spectral Frequency*. Monitoring of well-know upwelling spectral features shows the AIRS frequency calibration has drifted slightly during the first year of operation. This variation is a fraction of what could be detected radiometrically.
- Section 5.3.2. *Stability of AIRS Radiometric Calibration*. Sea Surface Temperature (SST) derived from the AIRS 2616 cm^{-1} window channel has been extremely stable relative to the Real Time Global (RTG) SST operational analysis at 0.08K rms since 1 September 2002, but with AIRS biased cold by 0.65K. About 0.35K of this cold bias was expected due to skin-bulk gradient and the day/night average of the RTG SST product (Aumann et al., 2003).
- Section 5.3.3. *Direct Radiance Comparison between AIRS and Aircraft-borne Instrument*. AIRS infrared radiances are compared with those from the Scanning High-resolution Infrared Sounder for very clear conditions over the Gulf of Mexico. In the water vapor band around 6.3 microns the two instruments agree to within their measurement uncertainties of about 0.1 K.
- Section 5.3.4.1. *Comparison with Radiances Calculated from Oceanic Buoys.* AIRS radiances are compared to top-of-atmosphere radiances in two window

channels, using a split window atmospheric correction method applied to over a thousand clear AIRS footprints (Hagan and Minnett, 2003). The mean bias for night only conditions is -0.3ºC to –0.5ºC for the shortwave at 2616 cm^{-1} and from -0.1 to -0.2 K for the longwave region at 938 cm^{-1}, with standard deviations of 1.0 K (Hagan, 2003).

- Section 5.3.4.2. *Comparison with Radiances Calculated from Radiosondes.* AIRS radiances are compared with radiances calculated from dedicated radiosondes. Sonde profiles are supplemented with ECMWF model analyses at upper levels. General agreement to within about 0.5 K is seen in three spectral regions: the 15 and 4.3 micron carbon dioxide bands, and the 6.3 micron water vapor band.
- Section 5.3.4.3. *Comparison with Radiances calculated from ECMWF Analyses.* A set of about 10,000 clear nighttime AIRS spectra taken over ocean in September 2002 are compared with radiances calculated from ECMWF analyses. The difference in the infrared window (about 800 to 1000 cm^{-1}) region is roughly 0.1 K when a known cold bias of about 0.5 K from ocean diurnal skin effect is considered. Other spectral channels originating in the lower troposphere show similarly good agreement. Poorest agreement is seen with humidity channels originating above about 500 mb, and also upper level temperature channels; in both these cases the disagreement is likely due to known problems with the ECMWF model at upper levels. The biases in the match-ups of AIRS window channels with buoys are generally consistent with these findings, to within few tenths of a degree.
- Section 5.4. *Provisional Validation of Visible / Near Infrared Observed Radiances*. Vis/NIR radiance uncertainties vary from about 7 to 11%, with unknown biases dominating.
- Section 6.1. *Rejection by Comparison with Forecast SST*. Retrieval footprints having sea surface temperatures disagreeing with RTG SST by more than 3 K are rejected. Maps of rejected areas show that these retrievals are affected by stratus clouds, dust, cirrus, scene inhomogeneities, and clouds that lead to degenerate solutions in cloud clearing. Understanding these effects are active areas of research.
- Section 6.2. *Beta Validation of Cloud-Cleared Infrared Radiances*. Cloud contribution to cloud cleared radiance uncertainties are estimated as a fraction of cloud amount by comparison with radiances calculated using ECMWF. This uncertainty varies from less than 1.0 K for little or no cloud to as much as 3.0 K for 70% cloudiness.
- Section 6.3. *Beta Validation of Sea Surface Temperatures*. Retrieved sea surface temperatures are compared with operational radiosondes, with ECMWF, and with an *Aqua* satellite-dedicated shipborne radiometer. These comparisons show a consistent difference of about -0.9 ± 1.0, so AIRS retrievals are biased cold. Roughly –0.5 K of this bias is due to diurnal ocean skin effects. The remainder of the bias and almost all of the standard deviation appears to be from propagation of cloud clearing errors into the retrieval.
- Section 6.4 *Provisional Validation of Temperature Profiles* Retrieved temperature profiles are compared with ECMWF analyses and with dedicated radiosondes. Root mean square errors over 1 km thick layers are 0.7 to 0.9 K throughout most

of the troposphere, becoming about 1.2 K at the lowestmost 1 km-thick layer. Biases are 0.2 K or less, with an oscillatory vertical structure. A slight improvement in retrieval quality is seen during nighttime, presumably due to weakened convective activity at night.

- Section 6.5 *Beta Validation of Total Water Vapor*. The global comparison with ECMWF shows an rms difference of 16.2%, with a bias of 0.01%. AIRS retrievals agree with operational sondes to 11.5% rms, with a bias of 2.9%. AIRS retrievals agree with dedicated sondes launched from the Chesapeake Light Platform by 10.6% rms, with a bias of 0.01%. Retrievals are biased by –10% against sondes launched from Nauru, the ARM Tropical Western Pacific site. The dry bias at Nauru is characteristic of the retrievals under very humid conditions; Nauru is in the most humid region on the planet. This dry bias dominates the rms error at Nauru of 11.4%. See Table 8.
- Section 6.6 *Beta Validation of Retrieved Water Vapor Profiles*. Some retrievals have a nonphysical 'kink' around 100 mb where the retrieved water vapor mixing ratio is fit to a stratospheric climatology. The AIRS retrieval does not currently provide information at this altitude, however. Retrieved water vapor profiles are compared against ECMWF and operation sondes. Biases with ECMWF are only 1 to 2 percent below 500 mb, but grow rapidly above. Root-mean-square errors against ECMWF are smallest --about 10%-- near the surface but increase to around 30% at altitude. See Table 9. Biases against operational radiosondes are –3.6 to 3.7% up to 350 mb, and rms differences grow from 11.6 to 50% with height. See Table 10.
- Appendix III *Beta Validation of Total Ozone*. Comparisons with TOMS satellite instrument observations show a difference of 4.4 ± 5.3%. AIRS retrievals show a large, positive bias off northwest Africa, possibly associated with lofted Saharan dust. A positive retrieval bias is also seen in the presence of high clouds.

3. Calibration, Forward Model, and Computational Uncertainties

Some of the factors contributing to retrieval uncertainty are described here. These are generally small, well-understood components of the retrieval error budget.

3.1. Calibration Uncertainties

The calibration errors of the AIRS instrument are well characterized and described in detail in Pagano et al. (2003), Strow et al (2003), and Gaiser et al. (2003). Noise equivalent brightness temperatures for AIRS channels used in the retrieval range from about 0.1 to 0.7 K, with a median of 0.18 K, at a reference temperature of 250 K.

The microwave instruments have known calibration errors due to uncharacterized sidelobes. See Sections 5.1 and 5.2 for an estimate of the sidelobe contributions to microwave radiance uncertainties.

3.2. Uncertainties in Forward Radiative Transfer Model

Forward radiance models are relevant to two parts of this report. First are comparisons between directly observed AIRS radiances and those calculated from in situ observations via those models. See Sections 5.1 and 5.2 for such comparisons in the microwave, and Section 5.3.4 for infrared comparisons. Secondly, forward radiance modeling is also central to the retrieval process, thus relevant to all of Chapter 6.

The uncertainties in the infrared forward model are described in Strow et al. (2003); see Figure 3 therein. Infrared model errors are general less that 0.1 K, though can exceed 0.2 K for a very limited set of channels, particularly in the 15 micron CO_2 band, the 9.6 micron 0_3 band, and the 6.3 micron H_2O band.

The microwave forward model uncertainties are described in Rosenkranz, 2003.

3.3. Computational Uncertainties in Retrieval

The retrieval process introduces several sources of uncertainty into the retrieved products. Simulations discussed in Fishbein et al. (2003) were used by Susskind et al. (2003) to estimate these errors sources.

4. Case Study

This section describes the comparison between an in situ correlative data set and associated AIRS quantities. The correlative data set consists of a radiosonde launched over the Chesapeake Light Platform at 6:30 UTC on 13 September 2002, a continuously, running cloud lidar also on the platform, and the European Center for Medium range Weather Forecasting ocean temperature analysis.

The East Coast of the United States was dominated by high pressure on 13 September 2002. This resulted on dry conditions throughout the area. This is readily apparent in Figure 2 where the dewpoint temperature is depressed by ten to twenty degrees throughout the troposphere. The lidar trace for this period (not shown) indicates a complete cloud-free sky for the two hours around the time of sonde launch.

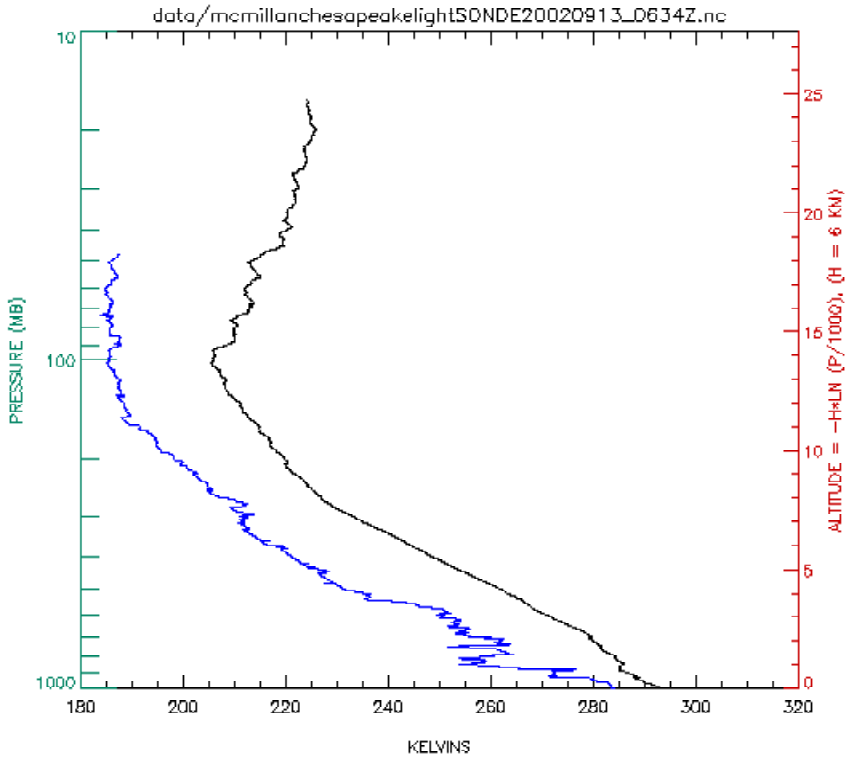

Figure 2 Temperature (black) and dewpoint temperature (blue) observed by radiosonde launches for Chesapeake Light Platform, 13 September 2002 at 6:30 UTC, 1:34 AM local time.

The sea surface temperatures for this day are shown in Figure 3. The Chesapeake Light Platform is a region of strong surface temperature gradients.

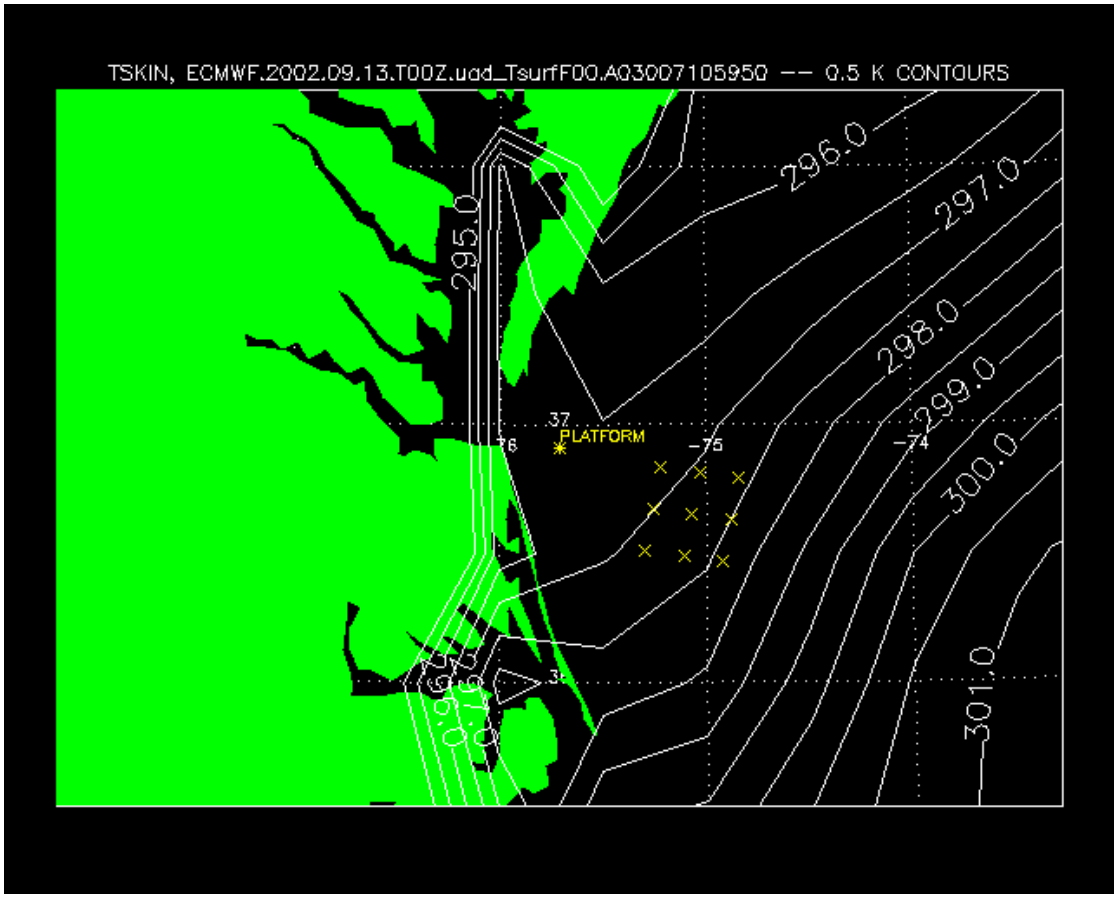

Figure 3. Surface skin temperature from ECMWF analysis, with platform location indicated the locations of 9 AIRS footprints marked.

Figure 4 shows the color-coded footprint locations and the directly observed AIRS spectra for the footprints marked in Figure 3. Note that the spectra are nearly identical to within about 1 K. Figure 5 shows the spectra in the 2600 to 2660 wavenumber portion of the same spectrum. This shortwave region is very clear, with water vapor opacities of order 0.1 K for this dry atmosphere. Comparing surface temperatures in Figure 3 with observed brightness temperatures Figure 5 shows that the warmest surface temperatures to the southeast are associated with the warmest AIRS observed brightness temperatures (blue and lavender). Conversely, the coolest radiances are observed in cooler, nearshore waters.

The differences between observed radiances and those produced by the AIRS forward model are shown in Figure 6. Here radiances are calculated using parameters from the sondes shown in Figure 2, and their difference from those radiances directly observed by AIRS are shown. The color-coding in Figure 6 indicates altitudes

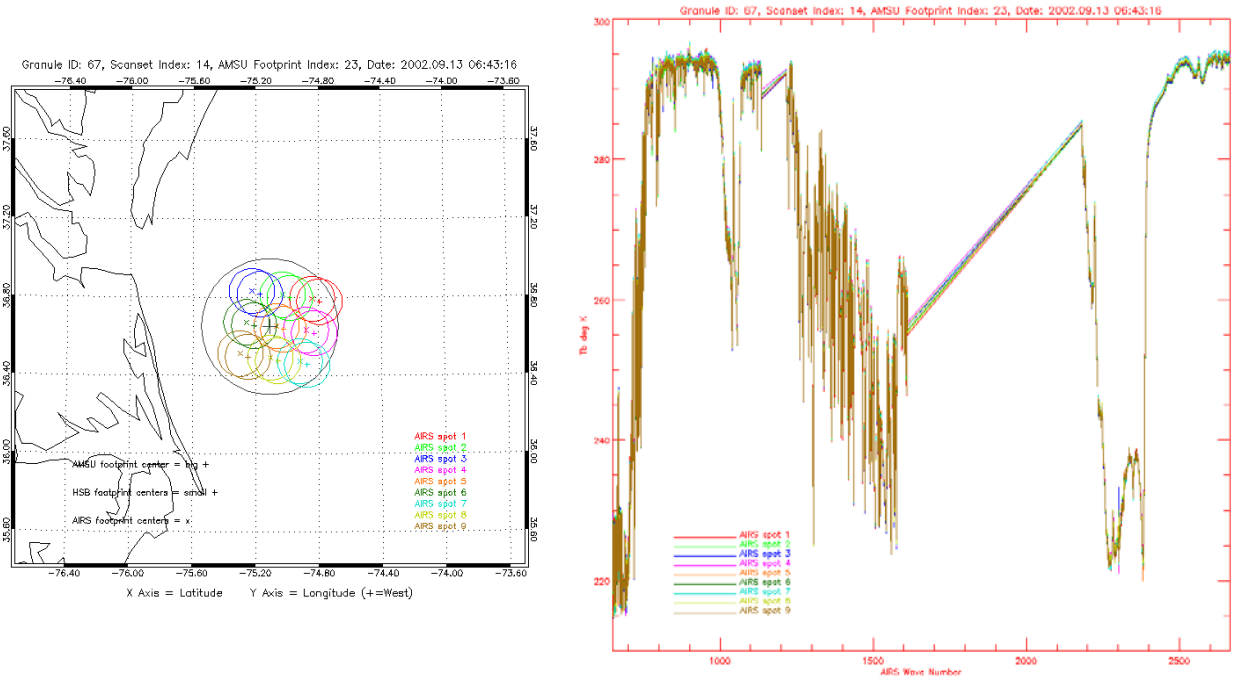

Figure 4. Color-coded locations marked in Figure 2, and associated observed AIRS spectra. The spectra are identical to within about 1 K; spectrum ordinate range is 210 to 300 K.

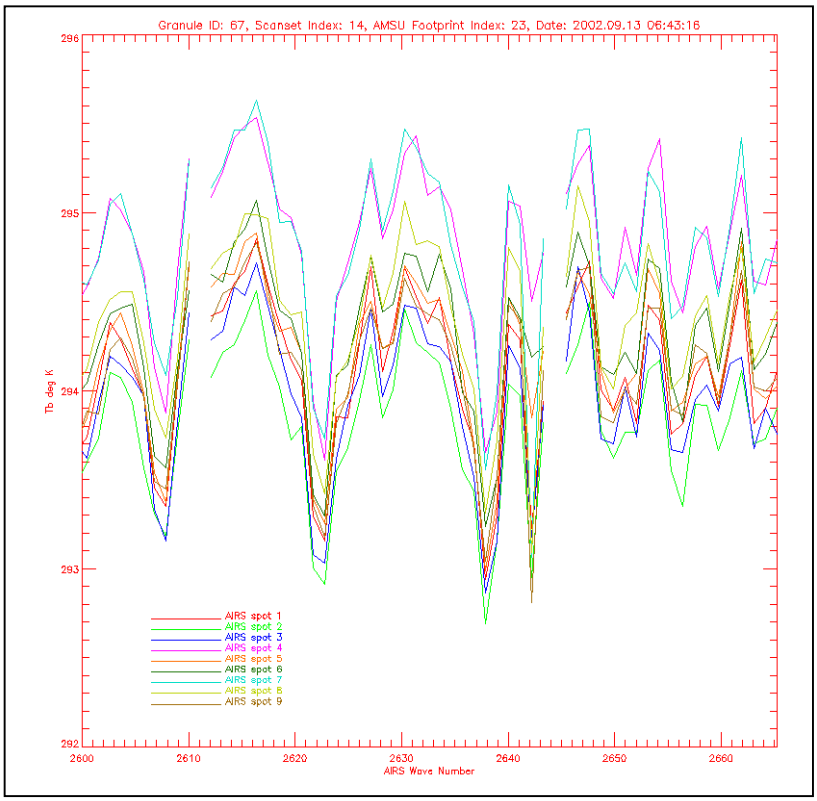

Figure 5. AIRS observed brightness temperatures at 2600 to 2660 cm^{-1}. Ordinate scale is 292 to 296 K.

of origin of the associated radiances. Red indicates channels whose weighting functions are below 400 mb, altitudes where the radiosonde observations are most reliable. Note that the differences for those channels marked in red are of order a degree or less. (Ozone, near 1000 cm^{-1}, is a special case since its weighting functions have a significant surface contribution while most ozone is concentrated in the stratosphere above 100 mb.)

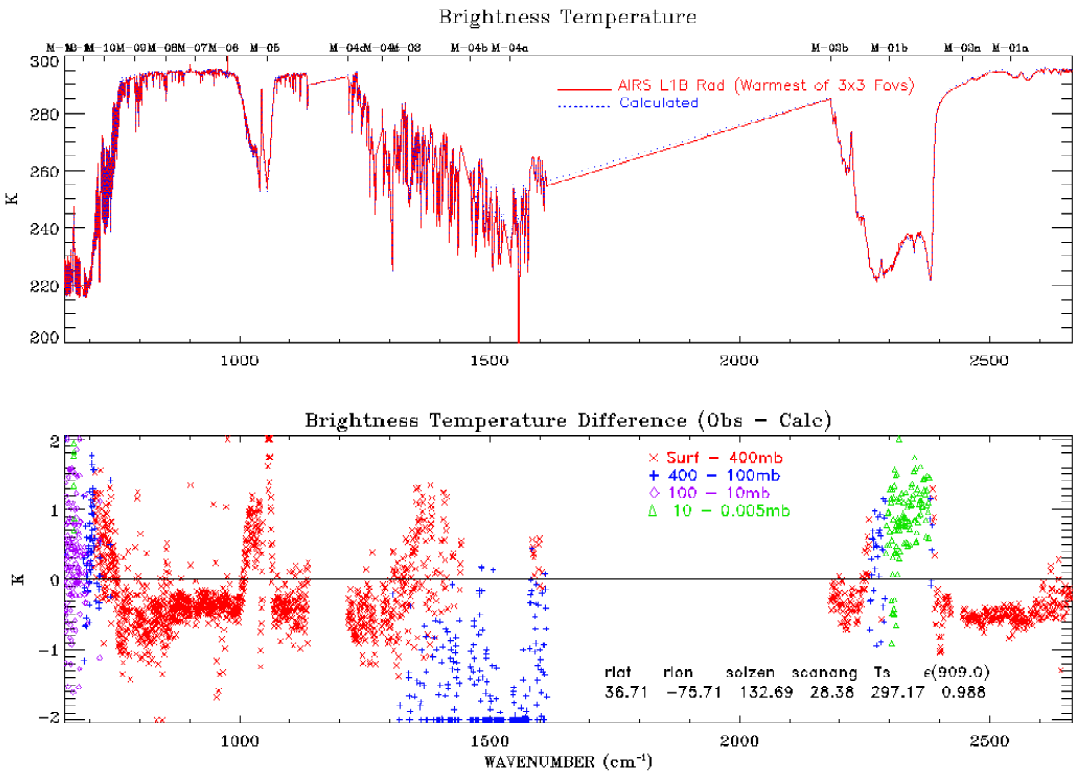

Figure 6. Observed and calculated AIRS spectra at locations shown in previous figures, using sonde observations (upper panel), and, difference between observed and calculated (lower panel). Color-coding in the lower panel indicates the pressure of the peak of the weighting function of the channel.

Figure 7 shows the difference between the AIRS retrieved temperature and radiosonde observed temperature, shown in Figure 2. The differences are less than 3 degrees absolute throughout the altitudes of observations.

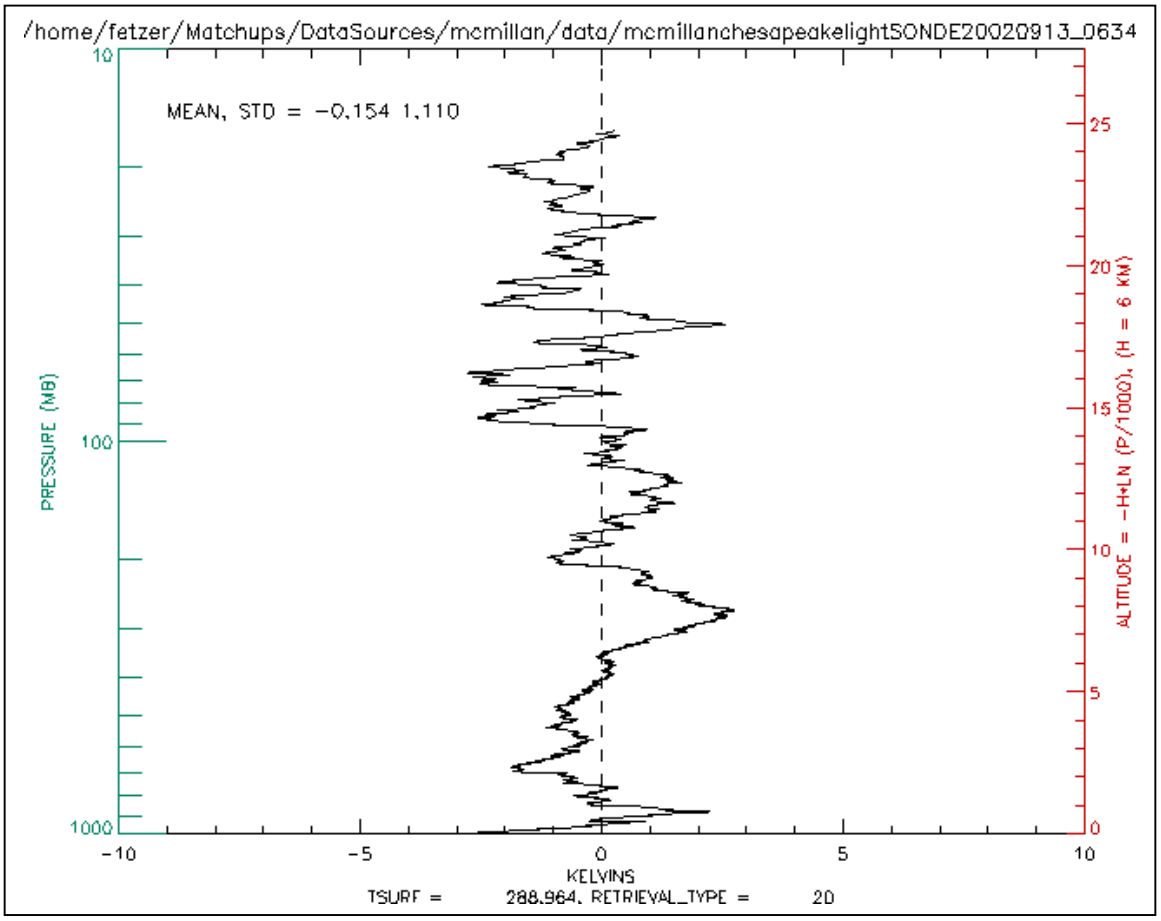

Figure 7. Difference between AIRS retrieved temperature and radiosonde temperature shown in Figure 2.

5. AIRS/AMSU/HSB Radiance Product Validation

This section describes the validation of directly observed AIRS / AMSU / HSB radiances. The microwave radiance observed by AMSU and HSB are validated at the Beta level (see Section 1.2 above definitions), while the AIRS infrared and Vis/NIR radiances are validated at the Provisional level. The microwave radiances are known to be affected by sidelobes viewing cold space. The result is a cold radiance bias. The sidelobe contributions are discussed below.

5.1. Beta Validation of Advanced Microwave Sounding Unit Observed Radiances

This section describes biases and variances in AMSU channels 4, 5, 6, 8, and 9 compared to radiances calculated from radiosondes. Channels 10-14 of AMSU are not computed from radiosondes, because their weighting functions peak too high in the atmosphere. AMSU Channels 1-3 and 15 receive substantial emission from the surface. Different validation techniques will be needed for these channels. AMSU channel 7 has excess noise equivalent to ~0.8 K, apparently due to interference from spacecraft transmitters, and is not used in the retrieval system.

AMSU requires some correction for the sidelobes that impinge on cold space. This adjustment was done here by first computing the ratio of observed antenna temperature Ta --including sidelobe contribution-- to calculated Tb using operational radiosonde profiles for four days: July 4, July 20, Sept. 6, and Nov. 29, 2002. A polynomial of degree 4 was fitted to these ratios, as shown for channel 6 as an example in Figure 8 (dither was added to the horizontal positions of data points to separate them when plotting). The fitted polynomials for five channels are plotted in Figure 9. Observed antenna temperatures were then adjusted by dividing them by the curves in Figure 9.

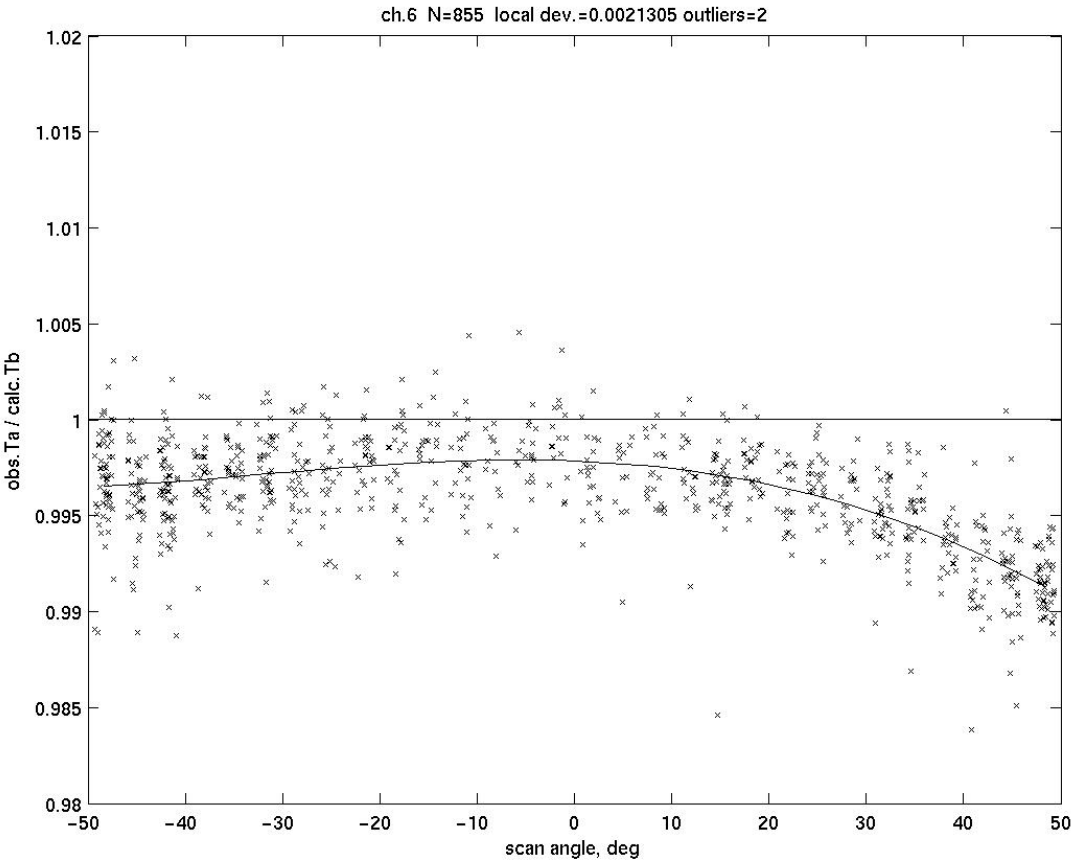

Figure 8 AMSU Channel 6 bias as a function of scan angle.

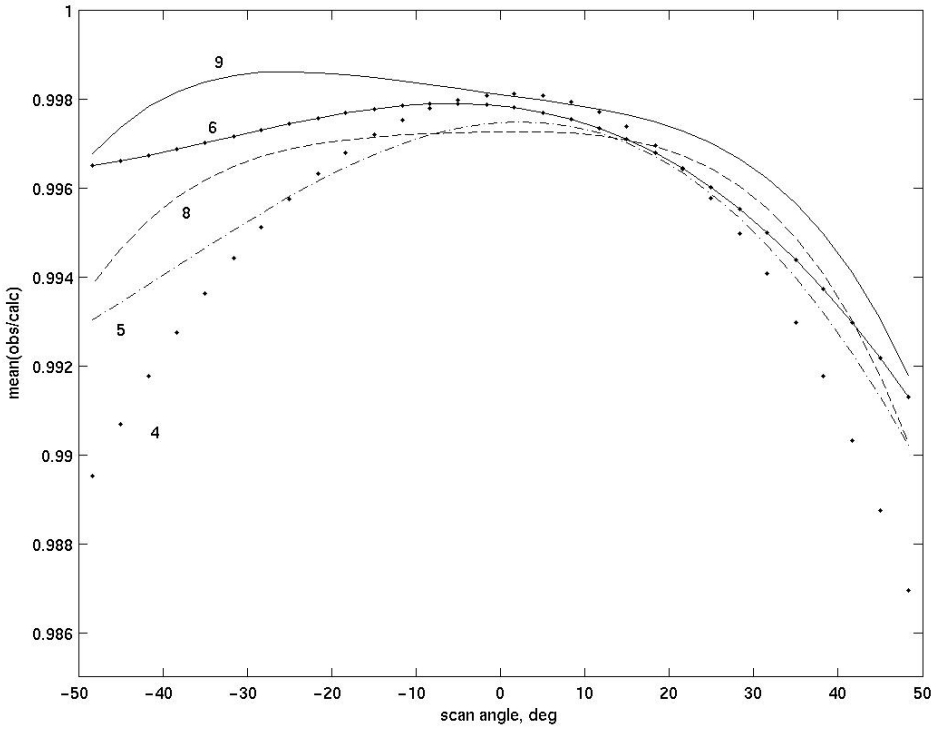

Figure 9 Polynomial fit to observations for five AMSU channels.

In Table 2, the adjusted brightness temperatures are compared to calculations from the dedicated coincident radiosonde launches from the ARM-SGP site in Oklahoma and from Guajara Mirim, Brazil. Hence, the small means shown in Table 2 for obs-calc represent differences between the operational and dedicated radiosonde datasets. Channel 4 has some contribution from the surface, which is difficult to model precisely. For further discussion of the method of calculation of Tb, see section V-B in Rosenkranz (2003).

Channel	Frequency, GHz	N	mean(obs-calc), K	σ(obs-calc), K
AMSU 4	52.80	93	0.346	0.758
AMSU 5	53.596	91	0.066	0.492
AMSU 6	54.40	88	-0.094	0.333
AMSU 8	55.50	81	-0.276	0.293
AMSU 9	57.29	52	-0.122	0.306

Table 2 Observed (adjusted) minus calculated Tb for AMSU, ARM-SGP & Guajara Mirim.

5.2. Beta Validation of Humidity Sounder for Brazil Observed Radiances

The validation of HSB channels 3, 4 and 5 is described here. HSB channel 2 senses the surface, precluding radiosonde comparison, and there is no HSB channel 1. The HSB instrument malfunctioned on February 5, 2003, and as of July 2003 has not been restarted

Channel	Frequency, GHz	N	Mean (obs-calc), K	σ(obs-calc), K
HSB 3	183.3 +- 1	60	-0.896	2.205
HSB 4	183.3 +- 3	59	-0.469	1.243
HSB 5	183.3 +- 7	59	-0.274	0.990

Table 3 Observed Ta - calculated Tb for HSB, ARM-SGP.

Table 3 contains the HSB biases and standard deviations of differences with ARM Southern Great Plains radiosondes. The sonde radiances are calculated with a microwave forward radiative transfer model for the sonde-observed temperature and humidity conditions. No correction for sidelobes has been applied to the HSB measurements. HSB channel 5 is shown in Figure 10. In principle, the antenna pattern should be the same for the three channels near 183 GHz, so the figure suggests that HSB may not need much, if any, correction for sidelobes. For these water-vapor channels, the validation was done with profiles from ARM-SGP, where Vaisala RS-90 sondes were in use. The Guajara Mirim, Brazil sondes were Vaisala RS-80 sondes. A dry bias in the RS-80 has been noted in other experiments, but these profiles have not yet been corrected for this effect, so they are not included in the statistics for water channels.

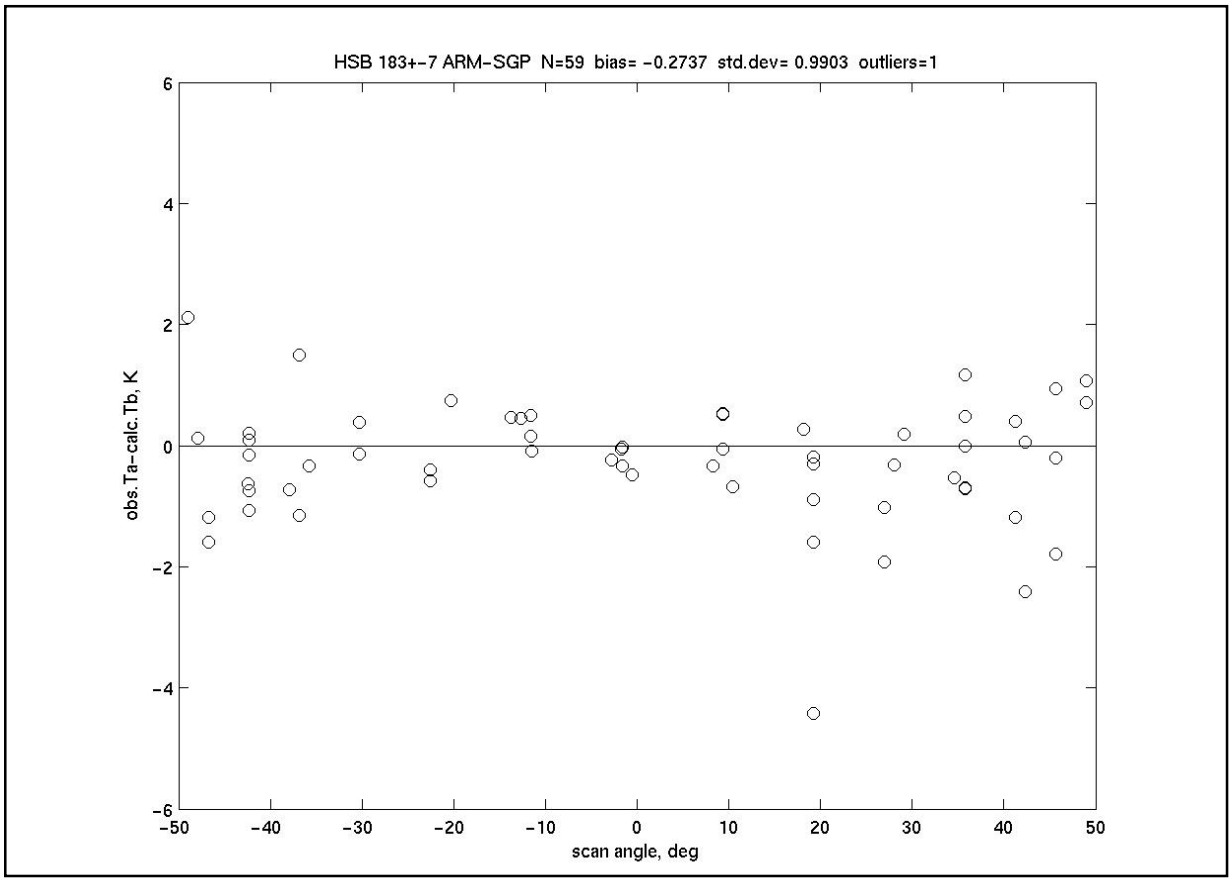

Figure 10 Scan biases for HSB

An alternate way to validate HSB radiances is by comparison with the corresponding AMSU-B observations obtained by NOAA-16 approximately 30 minutes later. Table 4 presents the mean differences between corresponding pixels for four granules representing ascending and descending passages over ocean on June 15 and Dec 15, 2002. Because the granule observed while ascending in June was affected by cloud liquid water varying over short times or distances, the affected pixels were omitted if their brightness temperatures were below 281, 241, 259, and 271K for HSB channels 2-5, respectively. Only the 10 or 11 scan angles best observed by both instruments were compared because the two swaths are not perfectly aligned. These comparisons suggest diurnal and seasonal differences between instruments are no more than several tenths of a degree.

	Channel 2		Channel 3		Channel 4		Channel 5	
	June	Dec	June	Dec	June	Dec	June	Dec
Mean bias (K), ascending	0.14	-0.26	0.25	0.57	0.16	0.50	0.29	0.49
Mean bias (K), descending	-0.04	-1.15	0.37	1.04	0.18	0.75	0.55	1.01

Table 4. Mean difference: [$T_{B\ HSB}$] minus [$T_{B\ AMSU\text{-}B}$] on NOAA-16 for single granules.

Table 5 presents the estimated rms deviations: 1) σ_{H-A} between HSB and AMSU-B single-pixel observations after the mean offsets are removed, 2) of all HSB channels (σ_H) measured before launch, as described in Lambrigtsen and Calheiros (2003); AMSU-B sensitivities were assumed to be the same, 3) $\sigma_{weather}$ contributed solely by changes in weather between the two observations 30 minutes apart, and 4) σ_{Hest} of HSB brightness temperatures estimated using bias-corrected AMSU-B observations from NOAA-16; $\sigma_{Hest} = (\sigma_{H-A}^2 - \sigma_H^2)^{0.5}$. To compute these values all four granules were averaged over the same pixels used for Table 4. Because HSB ceased operation in February 2003 there is interest in using NOAA-16 AMSU-B observations as proxy. The rightmost column in Table 5 presents σ_{Hest}, the inferred rms accuracy for HSB estimates based solely on bias-corrected NOAA-16 AMSU-B observations over ocean in the absence of significant liquid water clouds. The inferred increase, σ_{Hest} minus σ_H, is ~0.1 - 0.3K, but is sensitive to the assumed instrument noise levels and is degraded by liquid water clouds. It is degraded further by precipitation due to its strong variations in time and space. These accuracies σ_{Hest} are under study.

Channel		σ_{H-A}(K)	σ_H(K)	$\sigma_{weather}$ (K)	σ_{Hest}(K)
2	150 GHz	1.14	0.68	0.61	0.91
3	183±1 GHz	0.89	0.57	0.37	0.68
4	183±3 GHz	0.70	0.39	0.43	0.58
5	183±7 GHz	0.72	0.30	0.58	0.65

Table 5. Standard deviations of HSB relative to bias-corrected NOAA-16 observations.

5.3. Provisional Validation of Atmospheric Infrared Sounder Observed Radiances

This section describes some of the validation results supporting the Provisional validation status of directly observed AIRS radiances. See also Appendix III for a discussion of a large set of analyses performed by AIRS Science Team Members at the University of Wisconsin.

5.3.1. Stability of AIRS spectral frequency

The following discussion describes the long-term monitoring of AIRS spectral response. To summarize the results, AIRS has been stable at a detectable level since launch. Spectral drift is a very minor contributor to radiometric uncertainties, however.

Figure 11 shows a time sequence starting from beginning of stable frequency set through 10 months after launch. The method described here is intended to check for significant, unexplained trends from a near -13.5 micron value, if stable. (The –13.5 micron value is a reference focal plane position; other measurements in micron below also describe focal plane position.) Four upwelling spectral features were used, centered near 750, 1300, 1390, and 1605 wavenumbers. For each day, only granules with centers between +/- 30 degrees latitude were considered. (An AIRS granule contains 6 minutes, or 135 90-footprint wide scanlines.) From these granules, outliers were removed, and daily medians calculated. These are the values plotted.

A very slight trend is observed in Figure 11, from around -13.62 microns to -13.42 microns over the eight months plotted. This is a fraction of the 0.5 micron stability requirement, and much less than the 1+ micron change required before becoming detectable radiometrically. Thus a trend is detectable but is not significant. The cause of this trend is not understood. It may be real, or it may be an artifact of the spectral calibration method. If real, it may be due to changes in instrument thermal gradients or due to other unrecognized instrument change. It may also be due to changes in global atmospheric state, or due to instrument icing. Neither is the 'blip' in January 2003 understood.

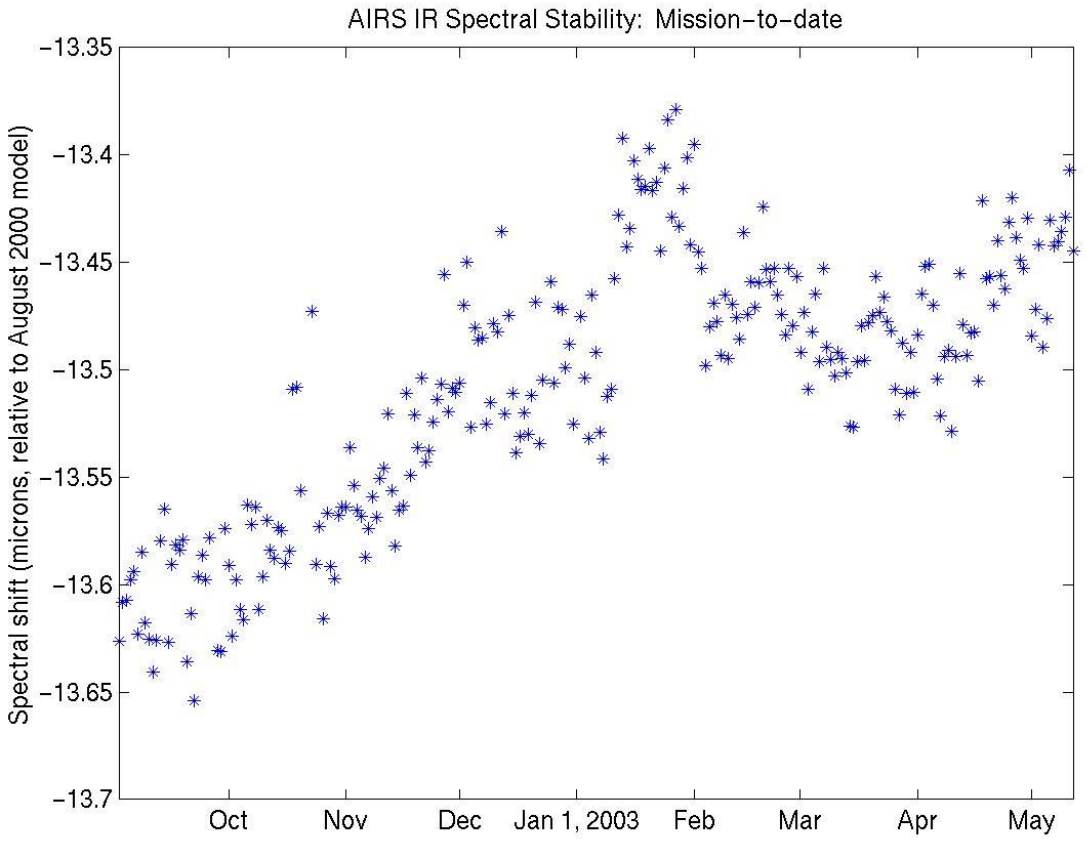

Figure 11. Spectral frequency relative to August 2000 zero point.

5.3.2. Stability of AIRS Radiometric Calibration

The following discussion describes the long-term monitoring of AIRS radiometric calibration relative to the RTG SST product (RTG.SST). To summarize the results, the SST derived from the AIRS 2616 cm^{-1} window channel has been extremely stable relative to the RTG.SST at 0.08K rms level since 1 September 2002, but with a cold bias of 0.65K (i.e. AIRS.sst2616-RTG.SST=-0.65K). About 0.35K of this cold bias was expected due to skin-bulk gradient and the day/night average of the RTG.SST. Details can be found in Aumann et al. (2003).

Figure 12 shows the result of the daily comparison of sst2616-RTG.SST starting from 1 September 2002 in terms of the bias (lower trace) and standard deviation (upper trace). The RTG.SST is carefully monitored on a daily basis relative to the buoys. The typical bias is less than 0.03K, with a standard deviation (of the population of about 200 buoys) of 0.4K. .

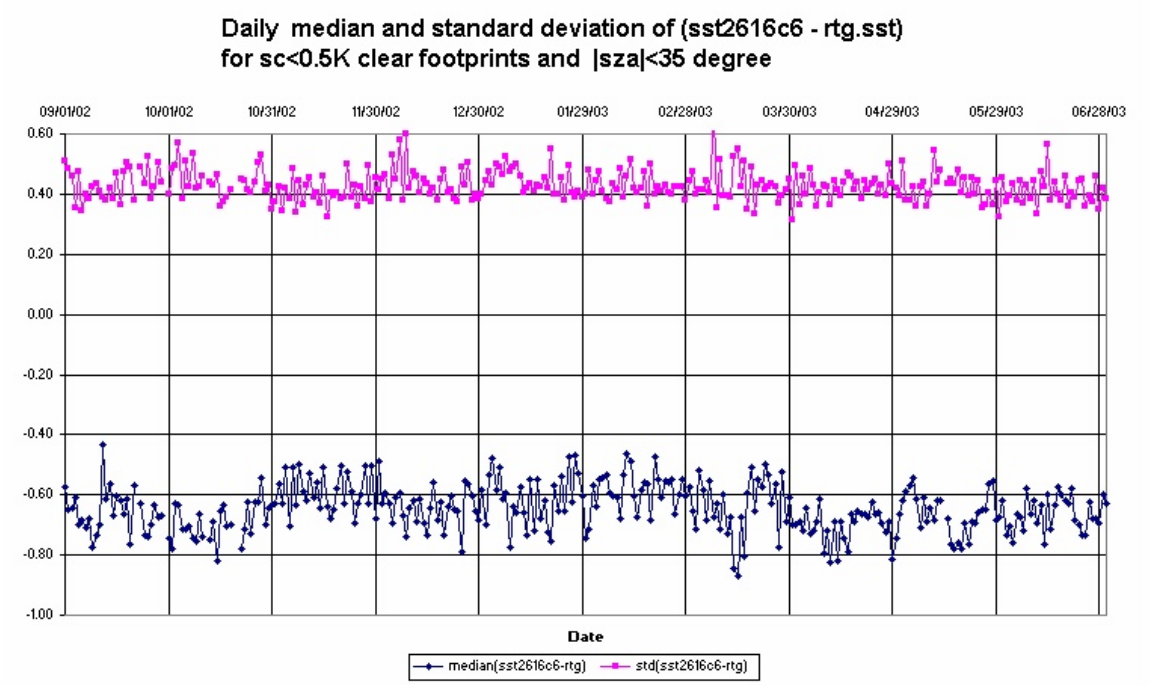

Figure 12. Time series of bias (upper curve) and rms (lower curve) between SST inferred from AIRS 2616 cm^{-1} channel and the RTG SST analysis. The statistics of the differences are summarized in Table 6.

For each day the sst2616 values, derived from the 2616 cm^{-1} window channel for about 8000 cloud-free night ocean footprints within ±50 degree latitude, are compared with the co-located RTG.SST product of the same day. This comparison results in a median difference and standard deviation of the 8000 points. The standard deviation is very stable at about 0.44K, and the median bias is 0.65K. The standard deviation of the bias for the first 10 months of data is 0.08K. There is no discernable seasonal trend in the bias. About 0.35K of this cold bias was expected: The RTG.SST is a day/night average product, and refers to the buoy temperature. The skin temperature at night is on average 0.17K colder than the buoy temperature. In addition, due to the diurnal surface warming, the RTG.SST is about 0.18K warmer at night than the buoys. The source of the remaining 0.3K bias is under investigation.

Within the ±50 degree latitude range the RTG.SST appears to be a very good product. In the following we argue that a deviation of more than 3K from the RTG.SST can be used as a first order quality check for the surface temperature retrieved from the cloud-cleared radiances. We analyze the quality of the RTG.SST product using the distribution of sst2616-rtg.sst for one month of data. A statistical summary of this analysis is given in Table 6. The distribution is approximately gaussian, but with a skew toward cold bias, mostly due to residual cloud contamination in a small fraction of "cloud-free" footprints. For a gaussian distribution with 0.41K standard deviation we would expect 98% of the population to be found between -1.65 K and +0.27 K (median+/-2.34*sigma), compared to the observed larger -1.9 to +0.36 K range.

However, only about one in 1000 RTG.SST matchups (283 in 269,134) is a 3K outlier. This infrequency argues that 3K can be used as a fair quality check threshold.

Total number of sst616-rtg matchups	269,134
Median difference	-0.69 K
Standard deviation of difference	-0.41K
98% population range	-1.9K to +0.36K
Number of points more than 3K warm	0
Number of points more than 3K cold	283 of 269,134
Number of points more than 5K cold	85 of 269,134

Table 6. Statistical summary of comparison between AIRS sst2616 and SST from RTG.

5.3.3. Direct Radiance Comparison between AIRS and Aircraft-borne Instrument

Figure 13 below shows a radiance intercomparison between AIRS and the Scanning HIS instrument, flown on the high altitude Proteus aircraft, over the Gulf of Mexico on November 16, 2002. These measurements were taken under very clear conditions. The spectra were pre-filtered by reconstructing them from a finite number of principal components to eliminate detector 'popping' in both instruments. This comparison makes no attempt to account for view angle, altitude, or scene differences. Nevertheless, the two instruments show excellent agreement to within the measurement uncertainties of both instruments. More detailed information about this intercomparison is available in Appendix III below in the section titled 'Analysis of aircraft based infrared observations (S-HIS, NAST-I) for radiance validation.'

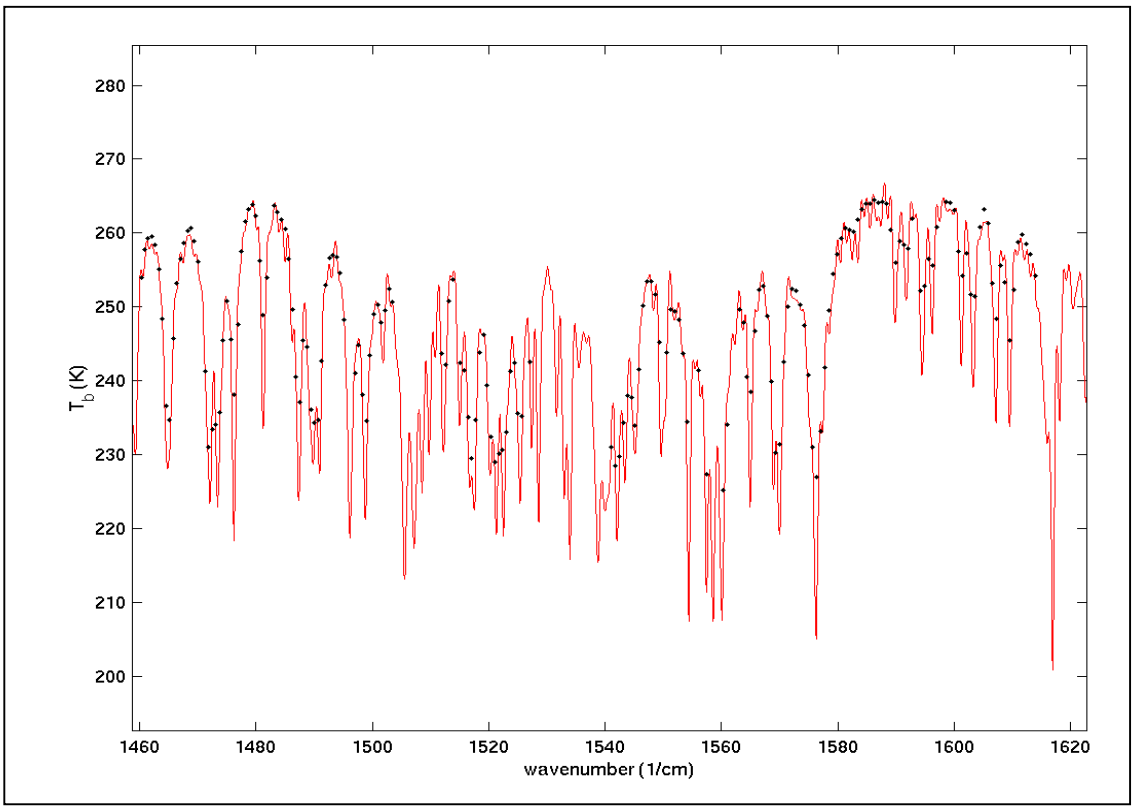

Figure 13. Comparisons between AIRS (black dots) and Scanning-HIS (red line) over the 1460 to 1620 cm^{-1} spectral region in the water vapor band.

5.3.4. Comparison between AIRS-observed and Forward Calculated Radiances

This section describes the result of comparisons between directly observed AIRS radiances and those calculated from other observations. This calculation requires the use of a forward radiative transfer model, so some of the errors in this intercomparison come from that model. The known radiative transfer model uncertainties are described above in Chapter 3. NOTE: The comparison with oceanic buoys in the next section is based on a split window atmospheric correction approach, which operates at a few wavelengths within the 800 – 1000 cm^{-1} spectral region.

5.3.4.1. Comparison with Radiances Calculated from Oceanic Buoys

The data of Figure 14 through Figure 16 were derived from two months of AIRS clear-sky, night only observations compared to the NOAA Global Telecommunications System (GTS) drifting buoy measurements co-located in space and time to within $\pm$50 km and two hours, respectively. These comparisons are made at frequencies where the atmospheric transmission is maximized (i.e., in window regions where there are no

discreet vapor phase absorptions, any residual absorption being due to diffuse [continuum] effects or to aerosols). A correction of the form

$$T\_surf(\upsilon)=BT\_{TOA}(\upsilon)+\alpha\sec(\theta) + \beta(\upsilon), \quad (1)$$

is applied to the observed TOA radiances to account for the reduction of the sea surface radiance by atmospheric absorption, and the effect of non-unity sea surface emission. The atmospheric correction term α, where θ is the instrument view angle, is determined from radiative transfer calculations using algorithms developed by Strow et al (2003) and Strow et al (2003a). The correction β was determined from the theoretical emissivity coefficients of Masuda et al. (1988). The dependence of emissivity on surface wind speed was not factored into the equation since the majority of observations described here were obtained for nadir angles less than 40^o. Based on 1400 match-up observations for the two month period, the mean global departures of AIRS observations from buoy SST measurements at night range from -0.3°C to –0.5°C for the shortwave region (2616 cm^{-1}) and from -0.1°C to -0.2°C for the longwave region (938 cm^{-1}) for data restricted to satellite viewing angles between +30 and -30 degrees.

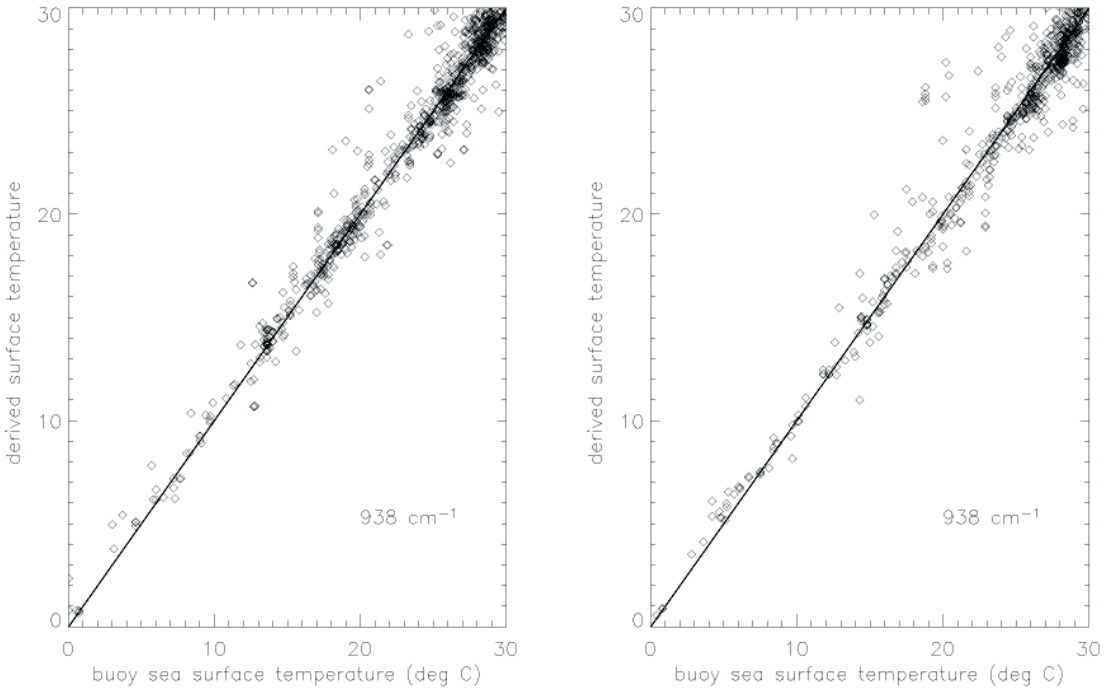

Figure 14. Scatter diagrams of buoy SST versus AIRS_SST_938 cm^{-1} (L1B TOA brightness temperatures at 938 cm^{-1} that have been corrected to the surface) for September 2002 (left) and October 2002 (right).

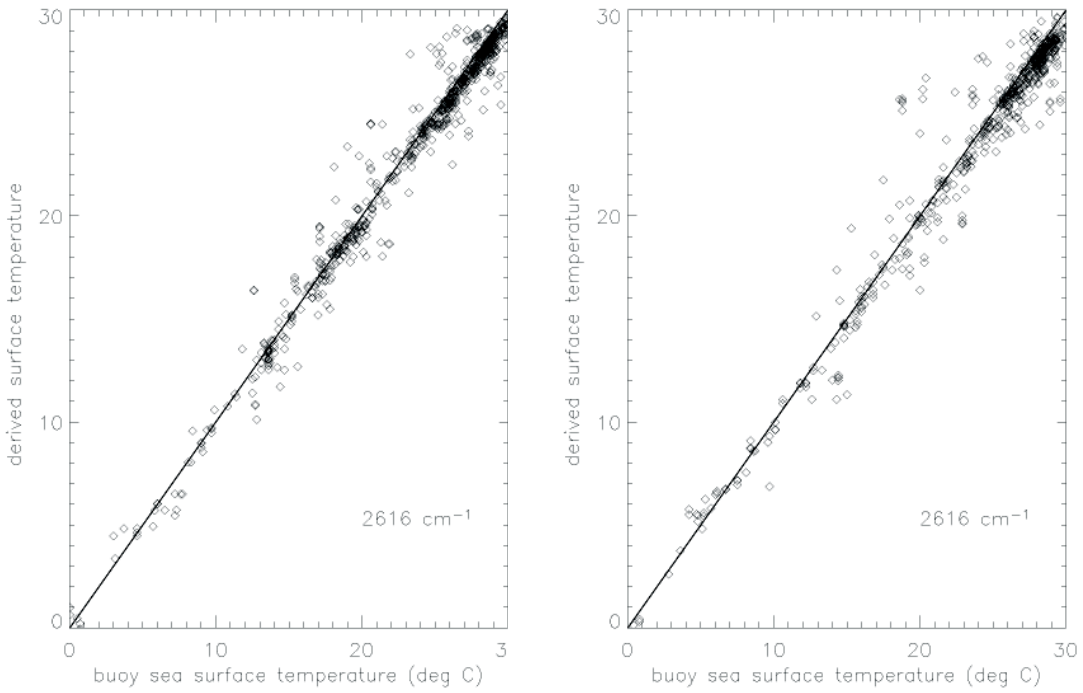

Figure 15. Scatter diagram of buoy SST versus AIRS_SST_2616 cm^{-1} (L1B TOA brightness temperatures at 2616 cm^{-1} that have been corrected to the surface) for September 2002 (left) and October 2002 (right).

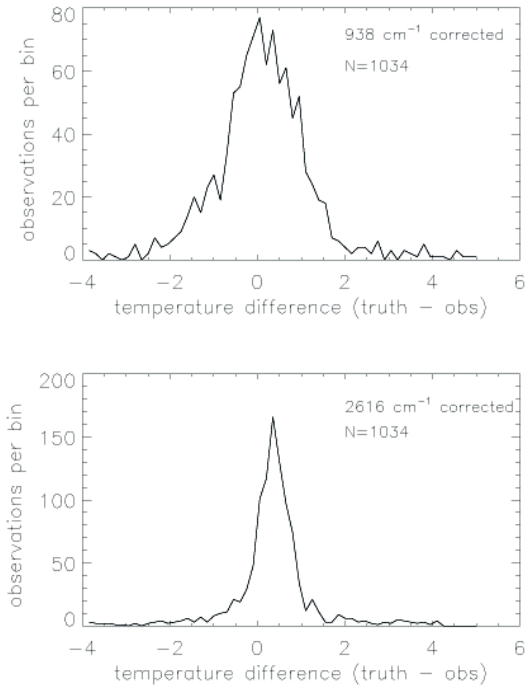

Figure 16. Histograms of the difference between buoy SSTs and AIRS derived surface temperatures, for global data restricted to satellite viewing angles between $+30^0$ and -30^0.

5.3.4.2. Comparison with Radiances Calculated from Radiosondes

The following comparisons show AIRS observed radiances relative to those calculated from AIRS-dedicated sonde. These comparisons utilize both land- and water-launched sondes (see Fetzer et al, 2003 for a map of dedicated site locations). The confounding effects of surface emissivity are avoided by comparing only at those wavelengths with insignificant surface contributions. Sondes are merge with ECMWF fields above the maximum altitude of sonde coverage.

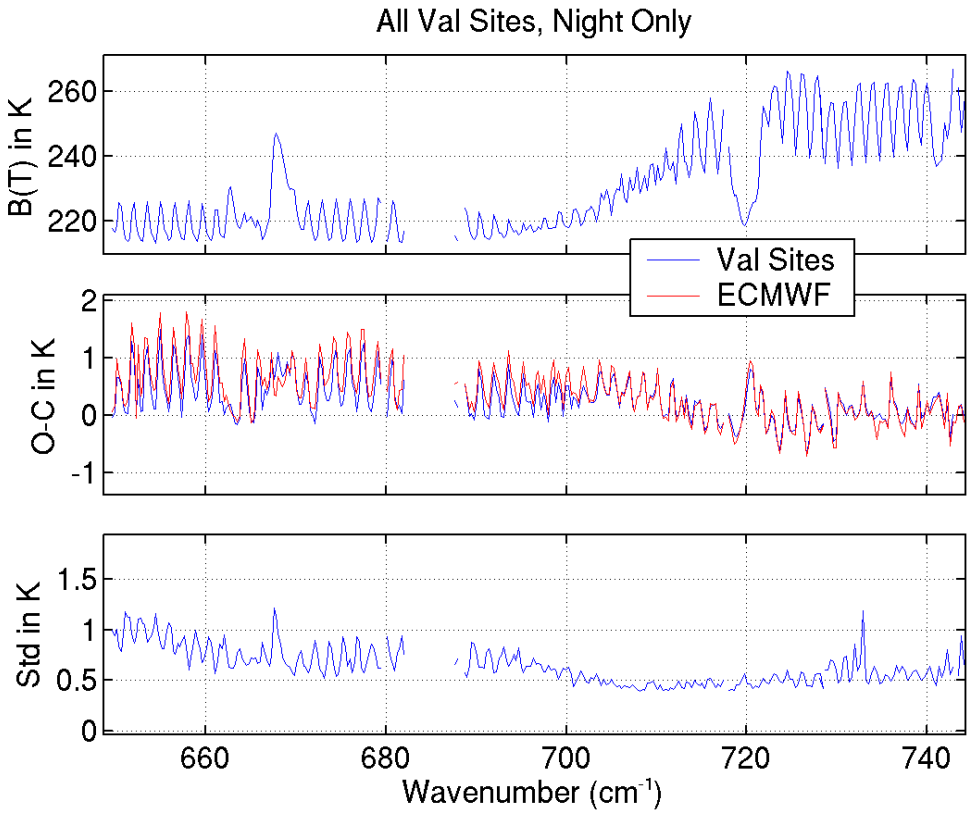

Figure 17. Top: Average AIRS-observed brightness temperature in the 645 to 760 cm^{-1} region at all AIRS-dedicated validation sites. Middle: Bias between AIRS and sonde-calculated (blue) and ECMWF-calculated (red) radiances. Bottom: Standard deviation of AIR-sonde differences. Higher biases as lower wavenumbers are due to a know problems with the ECMWF model.

Figure 17 shows the difference between AIRS sondes at the fixed sites in the 15 micron carbon dioxide band. A total of 134 sondes was used in this comparison. The biases between AIRS and ECMWF are also shown (see Section 5.3.4.3 for global comparison with ECMWF). The biases in the middle panel of Figure 17 are less than 1 K in the 710 to 745 cm^{-1} region. Higher biases at lower wavenumbers are due to known problems with the ECMWF model at higher altitudes, where no sondes are available so the model is the sole source of correlative information.

Figure 18 shows the AIRS-sonde and AIRS-ECMWF differences in the 6.3 micron water vapor band. Agreement between all three fields is good throughout most of the band. The bias at higher wavenumbers may be from a dry bias in the ECMWF water vapor at upper levels.

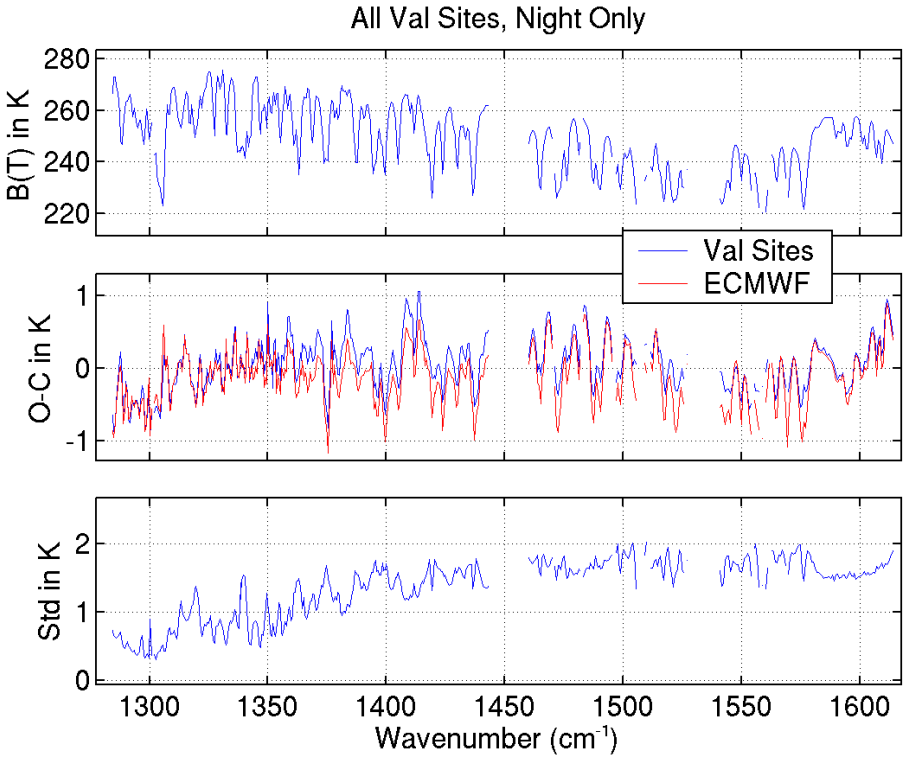

Figure 18. As in Figure 17 but for the 1280 to 1620 cm^{-1} spectral region.

Finally, Figure 19 shows the difference between AIRS and sondes in the carbon dioxide band around 4.3 microns. The agreement in most of these channels is good, but small systematic differences are under study, and may be due to scene-dependent effects.

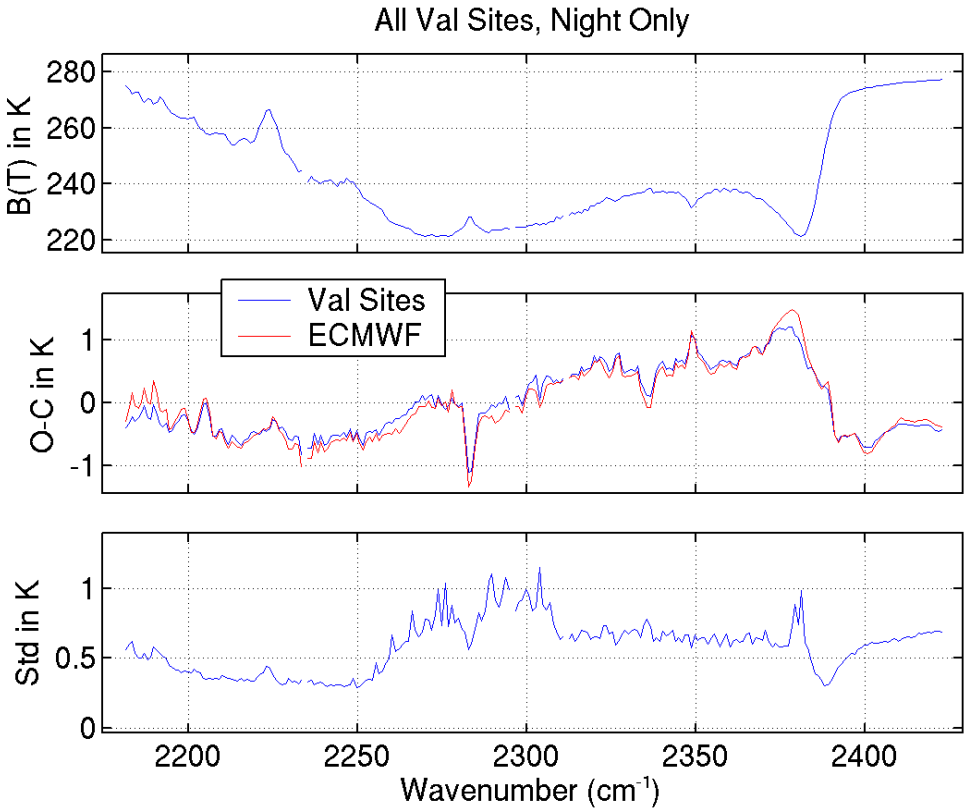

Figure 19. As in Figure 17 for the 2170 to 2430 cm^{-1} region.

5.3.4.3. Comparison with Radiances calculated from ECMWF Analyses

Comparisons with models offer the advantage of very large statistics, and very stringent selection criteria. In the following comparison only those oceanic nighttime fields of view that are nearly cloud-free are selected.

Figure 20 shows the mean clear-sky brightness temperature for AIRS, and the associated errors in AIRS radiances compared to the ECMWF quantities. The statistics are taken against 10,000 spots from September 2002.

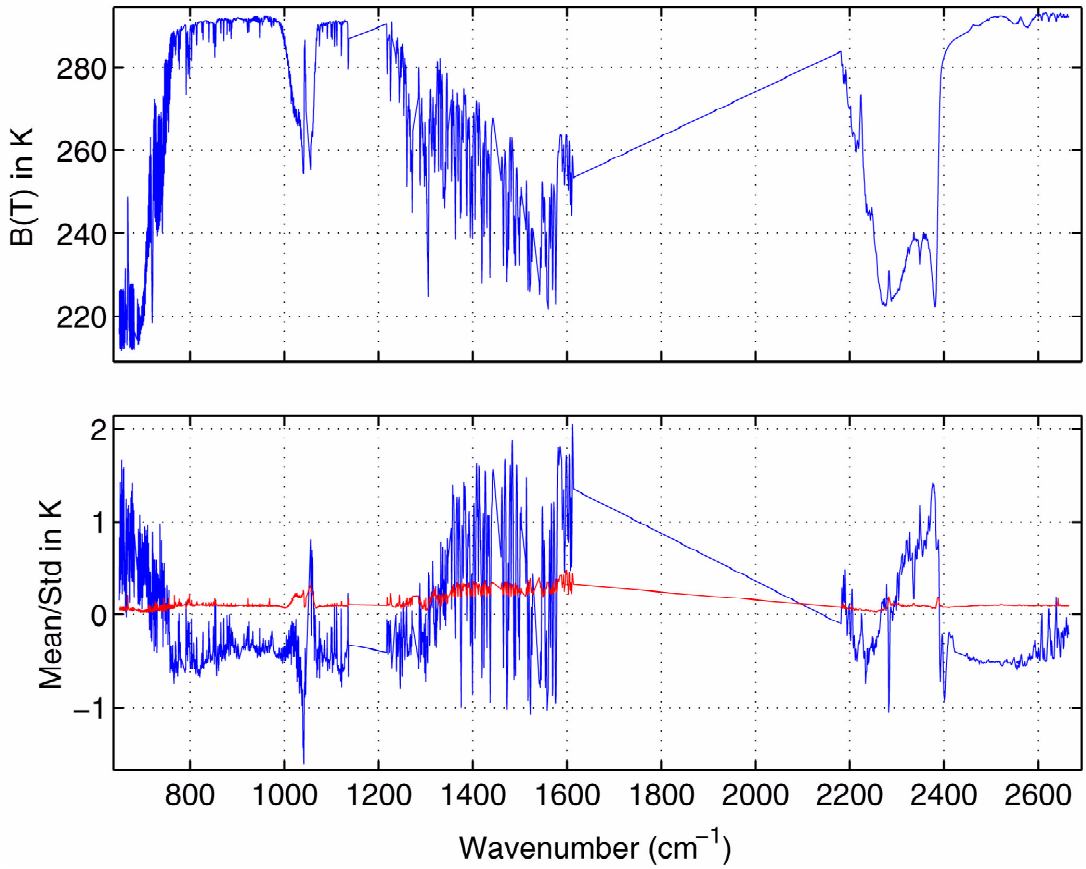

Figure 20. Mean oceanic nighttime clear-sky brightness temperature and associated errors, for September 2002. Red is bias and blue is standard deviation.

5.3.4.4. Thin Haze and Comparison with Model SST at 2616 cm^{-1}

The AIRS instrument has a shortwave channel at 2616 cm^{-1} with water vapor attenuation to the surface of order 0.25 K. This is the lowest water vapor attenuation anywhere in the infrared spectrum sampled by AIRS; for comparison water vapor attenuation is 1-2 K in the longwave window channels around 800-1000 2616 cm^{-1}. Thus, brightness temperature at 2616 cm^{-1} is the effective temperature of the cloud or surface being viewed.

The upper panel of Figure 21 gives average nighttime brightness temperatures at 2616 cm^{-1} for very clear footprints during September 2002 to February 2003. (This wavelength is significantly affected by reflected solar radiation during daytime). The corresponding difference with the Real Time Global SST analyses is shown in the lower panel. Note persistent cold bias in the difference. It can be nearly 2 K over large regions. While some of this signal may be due to cloud 'leakage', its persistence suggests a globally distributed attenuator at 2616 cm^{-1} due to aerosol or haze. The optical depth for a haze layer needed to explain a 0.3 K cold bias is of order 0.001.

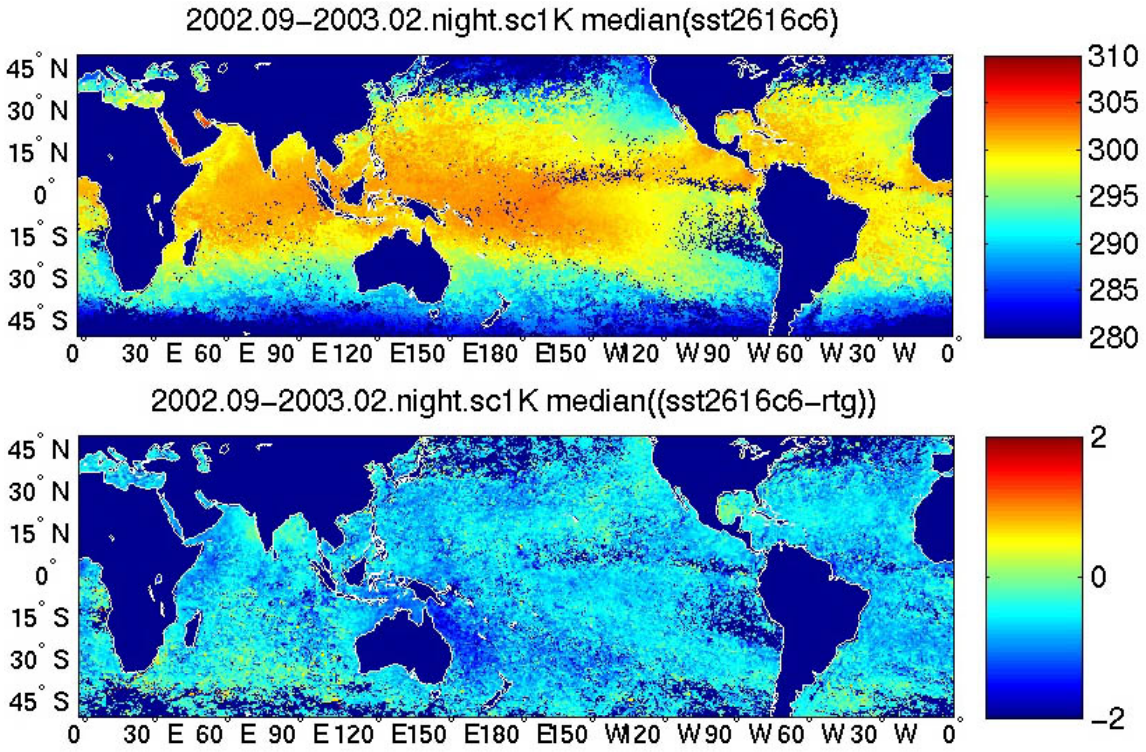

Figure 21. Upper: AIRS nighttime brightness temperature at 2616 cm^{-1}, averaged over very clear scenes, September 2002 to February 2003. Lower: Difference with RTG SST.

5.4. Provisional Validation of Visible / Near Infrared Observed Radiances

The AIRS Vis/NIR instrument was vicariously calibrated at Railroad Valley Playa, Nevada, in June 2002. This activity has been reported in Hofstadter 2002 (AIRS Design File Memorandum 590-Revised, dated 27 September 2002). The uncertainties on the absolute radiances are found to be 7% for Channels 2-4, and 11% for Channel 1. (Better than the requirement of 20% on each channel.) Pixel-to-pixel relative uncertainties within a channel are much smaller, with one-sigma errors of 0.3% in Channels 2-4 and 1% in Channel 1. Average gains of the 9 detectors within each channel are 0.5470, 0.2208, 0.1723, and 0.1922 W m^{-2} $micron^{-1}$ $ster^{-1}$ per instrument count, for channels 1 to 4, respectively.

Short-term variations (from seconds to months) in the Vis/NIR system are tracked by an onboard calibration system, consisting of dark current measurements and observations of calibration lamps. These are described in Gautier et al. 2003. Determination of absolute instrument gains is done via "vicarious calibration" against known ground targets. In June and July of 2002, we coordinated with an existing MISR-Terra field experiment in Railroad Valley Playa to carry out our first calibration. We expect to repeat the measurements annually to validate the existing calibration and to track changes in instrument performance. A second field campaign is underway at the time of this writing, the summer of 2003. Preliminary analysis of data collected on 14 June 2003 agrees with the initial calibration, to the quoted error bars (10% on Channel 1, better than 7% on the others).

The calibration process consists of three parts: estimation of top-of-the-atmosphere (TOA) radiances from an instrumented test region in the Nevada desert; determination of instrument gains for the detectors observing the test region; determination of all detector gains relative to each other. The first step, calculation of TOA radiances, is carried out in conjunction with the MISR-Terra team. A field team carries out solar radiance, surface reflectance, and atmospheric opacity measurements during spacecraft overflights of a bright desert playa, and uses a radiative transfer forward model to estimate TOA radiances. The forward model has been compared to independent calculations made by AIRS team members at UCSB and the MODIS validation team based at the University of Arizona. The TOA calculation has an uncertainty of 10% in Vis/NIR Channel 1, and 5% in the other channels.

In the second step, the single detector in each Vis/NIR channel viewing the test area is assigned a gain yielding the radiance calculated in the first step. The field data cover a region approximately 1 km across, while the Vis/NIR footprint is approximately 2.3 km across. This mismatch is acceptable because the playa is relatively uniform in the test region. Visual inspection of the field site and the spacecraft data suggests the uncertainty added by the Vis/NIR footprint size is a few percent.

In the final step of vicarious calibration, the detector-to-detector relative gains within each channel are calculated. This is done by choosing large, relatively uniform regions in the Sahara and Kalahari deserts, and assuming the spatially averaged radiance seen by each detector is the same. This allows the calibration of the single detector that viewed the Nevada test region to be transferred to all other detectors of that channel. Using different test regions to calculate the relative gains yields typical differences of less than 1%, providing the basis for the relative accuracy quoted in the first paragraph of this section.

Table 7 lists the final gain determinations for the nine detectors of each Vis/NIR channel. This calibration also serves as our validation; the observed Vis/NIR radiances now match the most accurate available information (from the 2002 field campaign), and are consistent with a second data set (from the 2003 campaign) to within the quoted error bars. This validation will be refined in the future through additional field campaigns, and by refining detector-to-detector relative gain measurements using both bright and dark scene data.

Detector	Gain (W m^{-2} $ster^{-1}$ $micron^{-1}$ per count)			
	Channel 1	Channel 2	Channel 3	Channel 4
1	0.546789	0.219287	0.172192	0.192768
2	0.546550	0.219646	0.172358	0.192848
3	0.545936	0.219851	0.171731	0.192614
4	0.546007	0.220022	0.171502	0.192652
5	0.545903	0.220427	0.171879	0.192195
6	0.545664	0.221015	0.172338	0.191840
7	0.547264	0.221677	0.172380	0.191436
8	0.548600	0.222200	0.172600	0.191400
9	0.550227	0.222946	0.173572	0.191722

Table 6. Final Vis/NIR Gain Determination

Table 7. Final Vis /NIR Gain Determination

6. Retrieved Product Validation

ALL AIRS/AMSU/HSB RETRIEVED PRODUCTS ARE VALIDATED AT THE BETA LEVEL (SEE SECTION 1.2). DO NOT ASSUME THAT GLOBALLY DERIVED RESULTS APPLY TO ALL CONDITIONS.

The AIRS/AMSU/HSB retrieved products described the state of the atmosphere as inferred from the directly observed radiances. This inference process uses a retrieval software system (see Susskind, et al, 2002). The retrieval involves many nonlinear transformations, so the relationship between uncertainties in the observed radiances and retrieved quantities is not simple. The validation of retrieved products requires comparison with a wide range of model analyses and in situ observations. Because validation of the version 3.0 data release is restricted to oceans between 40S and 40N, we have been limited by the number of high-quality in situ measurements, particularly radiosondes. For this reason this section relies heavily on comparisons with ECMWF analyses and on dedicated radiosonde observations from a handful of sites.

Note that all AIRS/AMSU/HSB retrieved products are validated at the Beta level for the version 3.0 data release. This means that the following results are preliminary. Understanding these results, and improving the retrieval system accordingly, is the priority activity of the AIRS science team. *The AIRS retrieved products are validated for the following conditions:*

- *Full combined infrared and microwave retrieval ran to completion.*
- *Ocean only.*
- *Latitude range 40S to 40N.*
- *Agreement between retrieval and NCEP forecast SST to within 3.0 K. The motivation for this is discussed in the next section.*

6.1. Rejection by Comparison with Forecast SST

AIRS retrievals are rejected if they deviate from NCEP AVN forecast by more than 3.0 K. This section describes some presumed reasons for those rejections. This report addresses only those retrievals whose SST agrees with the NCEP forecast SST to with 3.0 K. The motivation for this rejection criterion is illustrated by Figure 22 and Figure 23 below, which show where AIRS retrieved SST differs from ECMWF analysis SST to within 3.0 K, (blue) and greater than 3.0 K (red). White regions show where the retrieval solution reverts to microwave only, indicating cloud cover of greater than 70%. (Results for NCEP forecast are virtually identical to those shown because both depend upon the RTG SST analysis.)

As these figures show, rejection by the SST criterion of 3 K is highly localized. Large regions of retrieval rejection occur off the west coasts of South America, Africa, and Australia. This is apparently due to persistent, low stratus in these regions, a conclusion corroborated by the shape of observed AIRS infrared spectra (not shown).

Stratus also introduces a diurnal cycle into the retrieval yields, with higher yields in daytime. Yields are 74% for the daytime versus 69% for nighttime for the figures shown, and other days are similar (not shown). These differences are consistent with more extensive stratus coverage at night.

Another known cause of retrieval rejection is dust. AIRS spectra from west of Africa on 6 September 2002 exhibit a strong silicate signature in the 800 to 850 wavenumber infrared spectral band. Dust is therefore a presumed contributor to the higher retrieval rejection rate over the Atlantic off West Africa. Yet another known cause of retrieval rejection is cirrus clouds (Kahn et al., 2003). Optically thick cirrus is the presumptive cause of retrieval rejection on the edges of the cloudy regions in the tropics and midlatitudes away from the subtropical stratus regions. Also, certain cloud configurations give inhomogeneous detector response, with consequent spurious temperature differences with frequency. Finally, certain types of clouds lead to degenerate retrieval solutions (Fishbein et al., 2003).

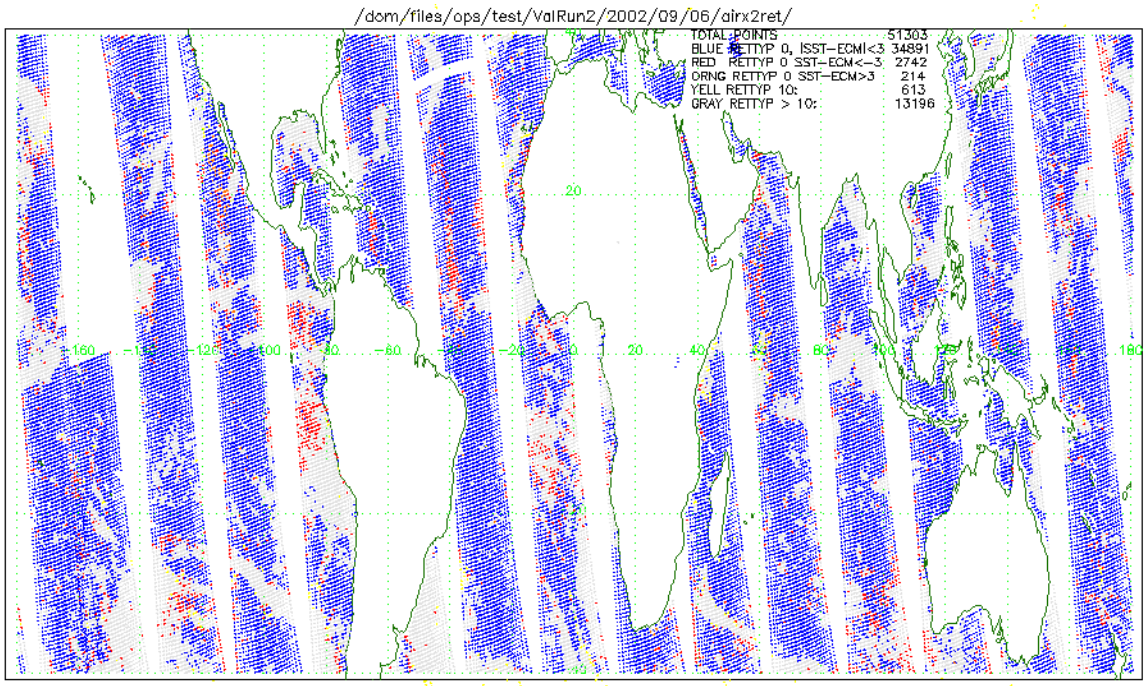

Figure 22. Daytime (ascending orbital node) locations where AIRS retrievals agree with ECMWF analysis to within 3.0 K (blue) and more than 3.0 K (red) for oceans between 40 S and 40 N, 6 September 2002. White gives those locations where the full AIRS retrieval reverted to microwave-only due to cloudiness greater than about 70%.

Note that more than one of these factors may be in effect simultaneously. For example, Saharan dust appears to be leading to retrieval rejection in regions of stratus near westernmost Africa, and of cirrus in the Bight of Benin. All three effects may be at play in some retrieval footprints off Africa. Similarly, both cirrus clouds and degenerate

cloud structures may both be leading to retrieval rejection along the edges of clouds in non-stratus regions. Disentangling these effects is an active area of research with the AIRS science team.

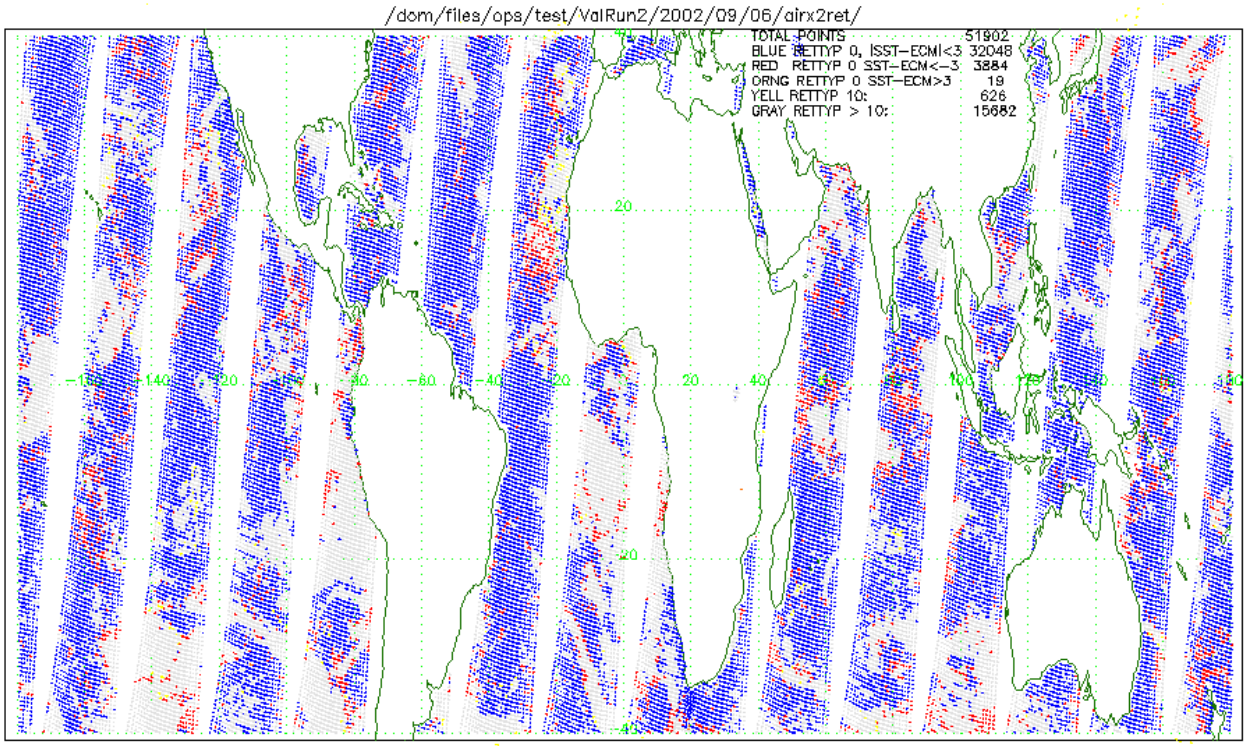

Figure 23. As for Figure 22, but for nighttime (descending orbital node).

6.2. Beta Validation of Cloud-Cleared Infrared Radiances

The magnitude of cloud clearing for retrieved cloud fraction of 40 to 50% is shown in the bottom panel of Figure 24. This value is calculated by calculating the average difference between cloud cleared and observed AIRS infrared radiances. Note that the largest amount of cloud clearing is in the window channels, with relatively small amounts at wavelengths originating higher in the atmosphere. See also Figure 26 below and associated discussion.

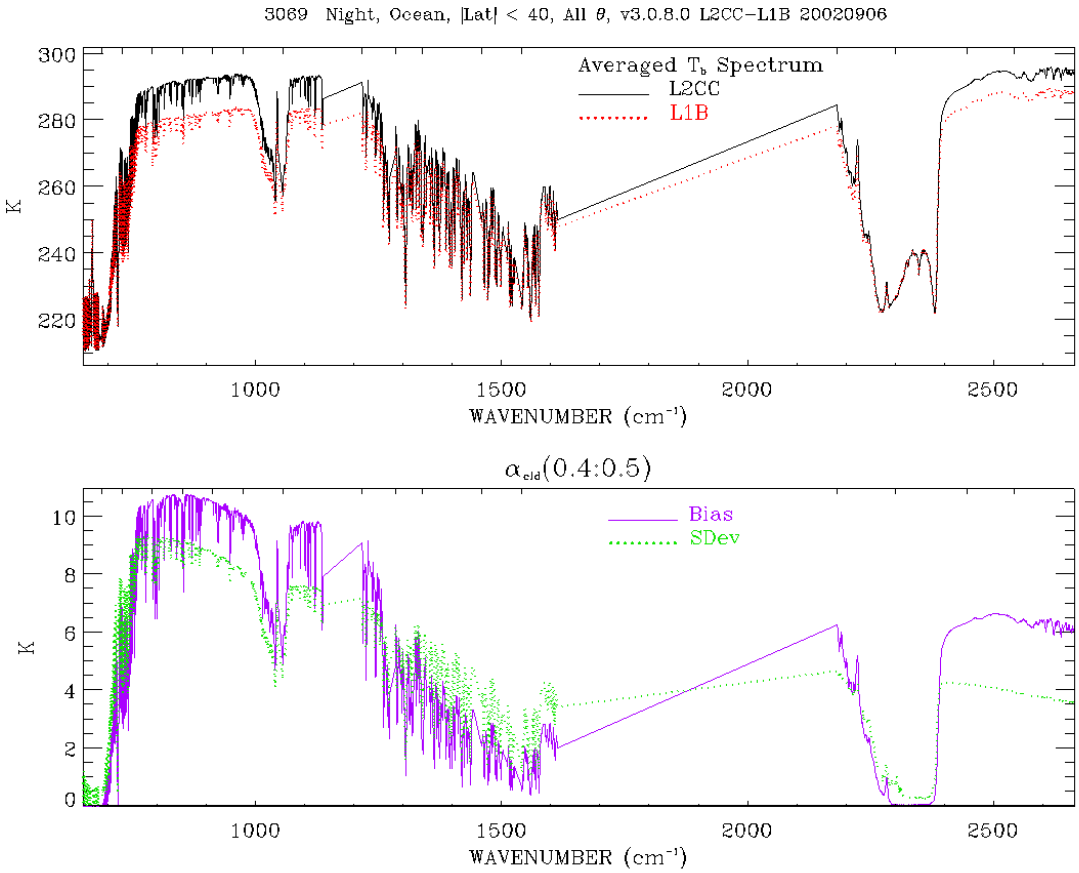

Figure 24. Difference between cloud cleared radiance and observed radiance for 3069 retrievals with retrieved cloud fractions of 40 to 50%. This is a measure of the effect of cloud clearing.

Cloud cleared radiance correlative observations are generated by calculating radiances with a forward radiative transfer model using ECMWF model fields as input, but not calculating the cloud contribution. This yields a large set of spectra for comparison with AIRS retrieved cloud cleared spectra.

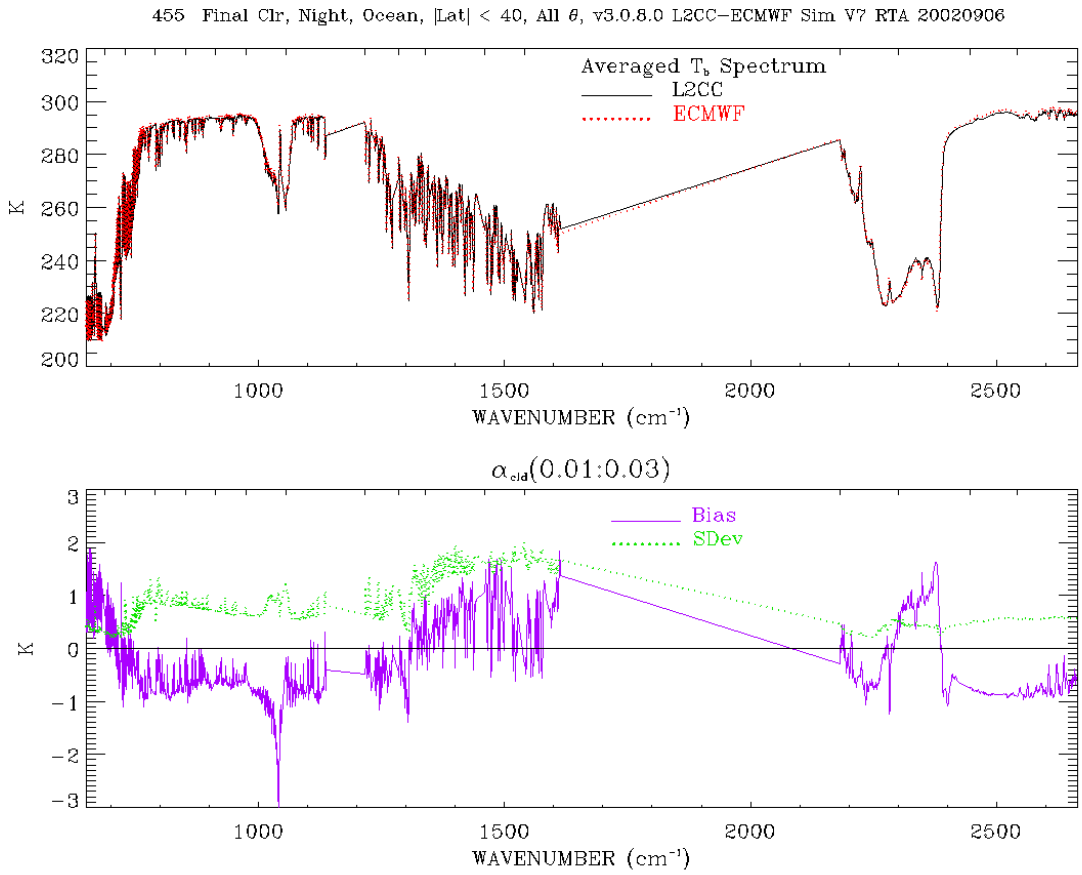

Figure 25. Difference between cloud cleared radiance and forward calculated clear-sky radiance from ECMWF for 455 AIRS retrievals of relatively clear cases with retrieved cloud fractions of 1 to 3%. Top, Mean brightness temperature spectra (cloud cleared -- black, calculated -- red); bottom, bias (purple) and standard deviation (green) of the differences.

The upper panel of Figure 25 shows the AIRS retrieved cloud cleared radiances and the ECMWF model calculated radiances on 6 September 2002 averaged over nighttime scenes whose retrieved cloud fractions are between 1 and 3%. The lower panel gives the mean, bias and the standard deviation of the difference. Restricting the comparison to nighttime reduces the effect of surface reflection and non-local thermodynamic equilibrium at shorter wavelengths. The cold biases of about 1 K in the window regions around 750-1000 and 2500-2650 cm^{-1} have three possible sources. First is a misrepresentation of model SST, known to be warm by roughly 0.5 K at night. The second possible cold bias source is AMSU sidelobes, discussed above. Finally, misidentified clouds are usually colder than the underlying surface, leading to a cold bias in cloud cleared radiances. Figures similar to Figure 25 for cloud fractions of roughly 10% to 40% are essentially identical, suggesting minimal cloud contribution for low cloudiness scenes. Errors from misrepresented clouds grow for cloud fractions greater than 40%, however, and can contribute up to 3 K rms for cloud fraction of 70 to 80% (not shown). Figure 26 shows the cloud clearing errors for cloud fractions of 40 to 50 %, where errors are about 0.2 K greater than those in Figure 25. So, given the known model

skin effects, the biases in the window region in Figure 25 are about 0.5 K, with an additional 0.2 K of bias introduced for cloud fractions in the 50% range in Figure 26. Compare the estimated error from cloud clearing shown in Figure 25 with the relative magnitude of cloud clearing shown in Figure 24 above.

Some spectral regions of Figure 25 and Figure 26 show systematic differences due to known model problems. Most notably, the water vapor bands around 1400 to 1600 and 2300 to 2400 cm^{-1} are biased warm. This is caused by a known dry bias in the ECMWF model in the upper troposphere. Similarly the cold bias in the ozone band around 1000 to 1100 cm^{-1} is from model misrepresentation of ozone, and the warm biases on the far left of the curve are from a cold upper stratosphere in the ECMWF model.

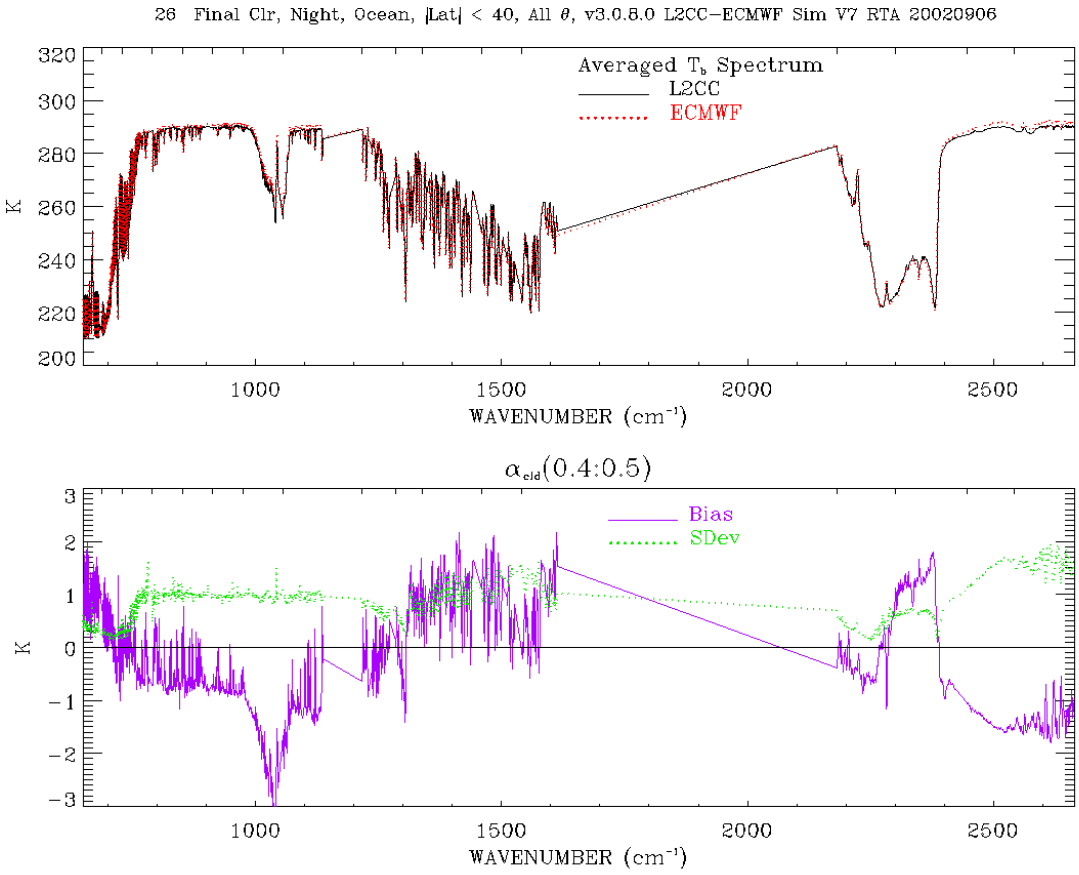

Figure 26. As in Figure 25, but for 26 AIRS retrievals with 40 to 50% of retrieved cloud fractions.

6.3. Beta Validation of Retrieved Sea Surface Temperatures

6.3.1. Comparison with Operational Buoys

Comparisons of AIRS Level 2 SST with global oceanic drifting observations are shown in Figure 27 and Figure 28. The figures show median differences for day and night binned as functions of latitude and scan angle for multiple days spanning the September through December validation period. The data show greater variability in the daytime bias for southern latitudes. This may be related to seasonal shifts in sunglint patterns to the south. The bias as a function of scan angle is larger during day than night. Overall, the bias of the temperature difference during day is on average -1.1 K, and at night –1.3 K with standard deviations of 2.0 K, but including those profiles differing from forecast by ±3 K. Rejecting these gives an average difference of –0.8 ± 1.1 K.

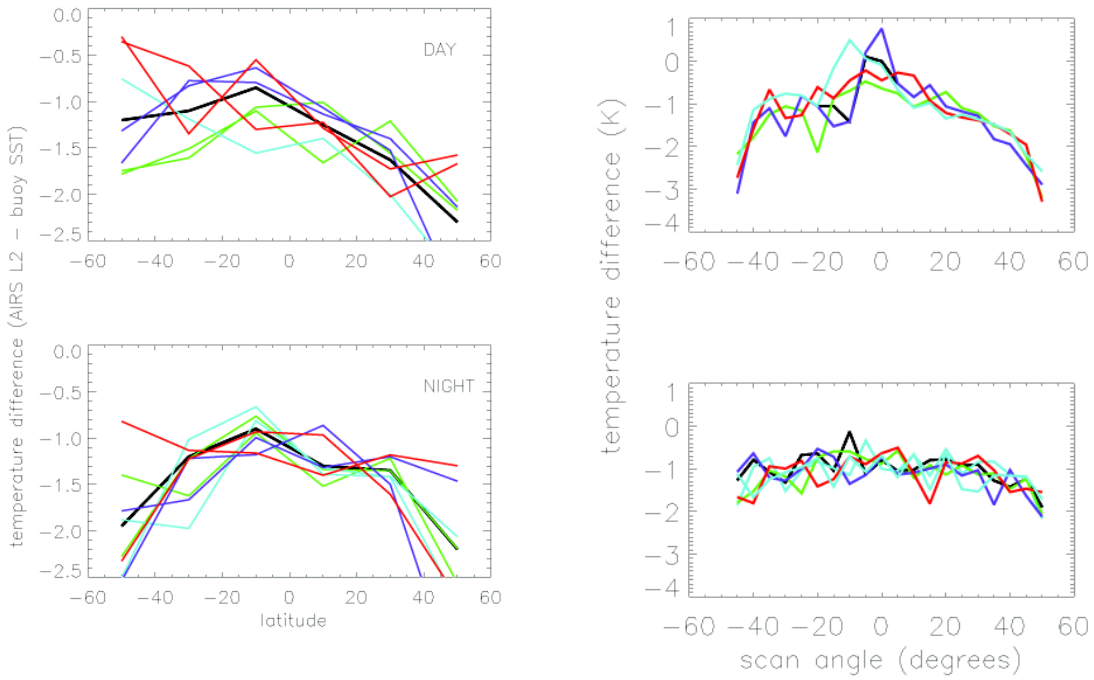

Figure 27. The dependence of (AIRS SST minus buoy SST) with latitude (left), and with scan angle (right) for 8 days during September through December 2002

For the same set of comparisons, the dependence of SST difference with temperature is shown in Figure 28. The graph shows patterns that are repeatable for tropical to subtropical temperatures of 20-30 ^{o}C, reaching a minimum temperature difference at about 25 ^{o}C, and a maximum temperature difference at about 20 ^{o}C. The variability is significantly greater for SST ranging between 10 and 20 ^{o}C.

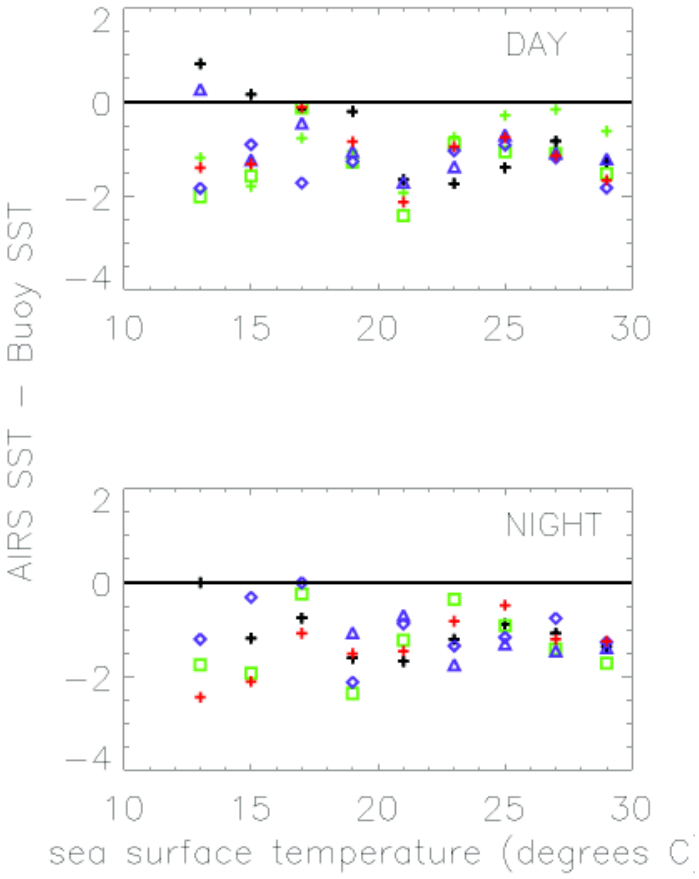

Figure 28. Global median temperature differences between AIRS SST and buoy SST as a function of buoy SST; six days between September and December 2002.

6.3.2. Comparison with Ship-borne Radiometer

Figure 29 shows the difference between AIRS SST and SST derived from the Marine-Atmospheric Emitted Radiance Interferometer (M-AERI) carried on a circuit of the Caribbean Sea by the *Explorer of the Seas* cruise ship (Hagan and Minnett 2003). Comparing this result with buoy observations in the previous section, note that the error here is -0.85 ± 1.2 K very similar to the –0.8 ± 1.1 K difference for operational buoys. NOTE: the M-AERI comparison includes all retrievals, whether or not they disagree with forecast. Also buoy data are based on global comparisons, the M-AERI statistics are based on regional data obtained at surface temperatures of 29 C, and include both day and night comparisons.

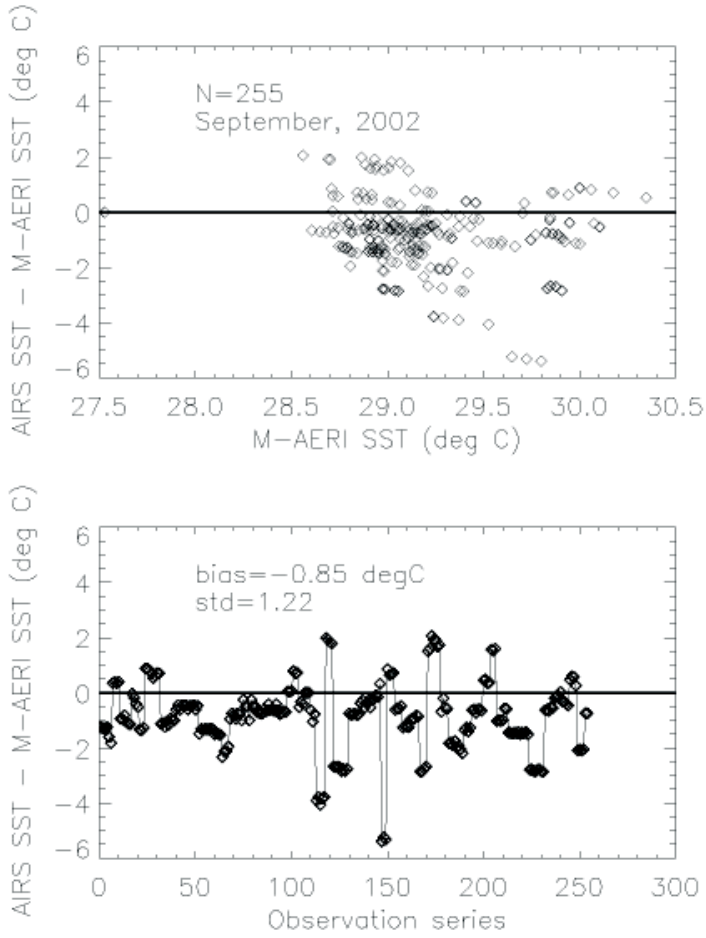

Figure 29. Upper: AIRS - M-AERI SST difference as a function of M-AERI-observed SST. Lower: difference as function of observation number, monotonic in time for September 2002.

6.3.3. Comparison with Model SST Analyses

Maps of SST differences between retrievals and ECMWF for 6 September 2002 are shown in Figure 30, and the associated distribution is shown in Figure 31. The cut-off at -3 K in the distribution is due to the 3 K rejection threshold discussed above. The global distribution of SST error is not uniform. The regions of high large error around 25 N are a known, contribution from sun glint; the solar reflection point is confined to these regions.

The truncated distribution in Figure 31 is caused by the constraint of ±3 K agreement with NCEP forecast SST, as discussed in Section 6.1.

The difference map and associated histogram for nighttime only conditions are shown in Figure 32 and Figure 33, respectively. Comparing the maps in Figure 30 and

Figure 32 show the contribution of sun glint to the daytime SST retrieval errors. Comparing histograms in Figure 31 and Figure 33 show the reduced number of large, positive outliers.

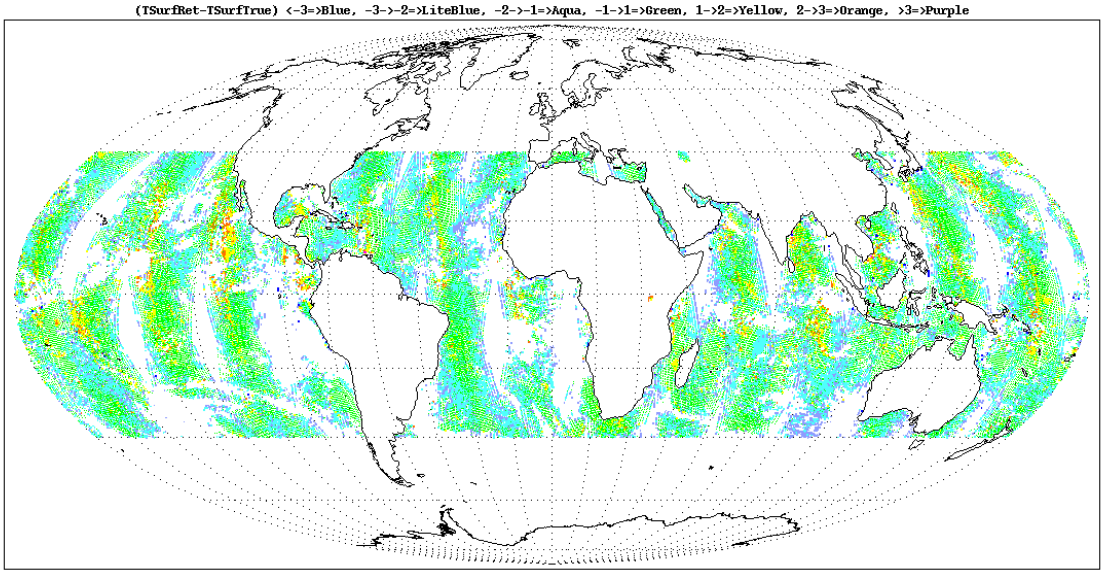

Figure 30. Combined day and night differences between retrievals and ECMWF SST for 6 September 2002. Colors are light blue: –3 to –2 K, aqua: –2 to 1 K, green: –1 to 1 K, yellow: 1 to 2 K, orange: 2 to 3 K. White areas indicated either retrieved cloud cover greater than 70% or retrieved SST deviating from forecast by more than 3 K.

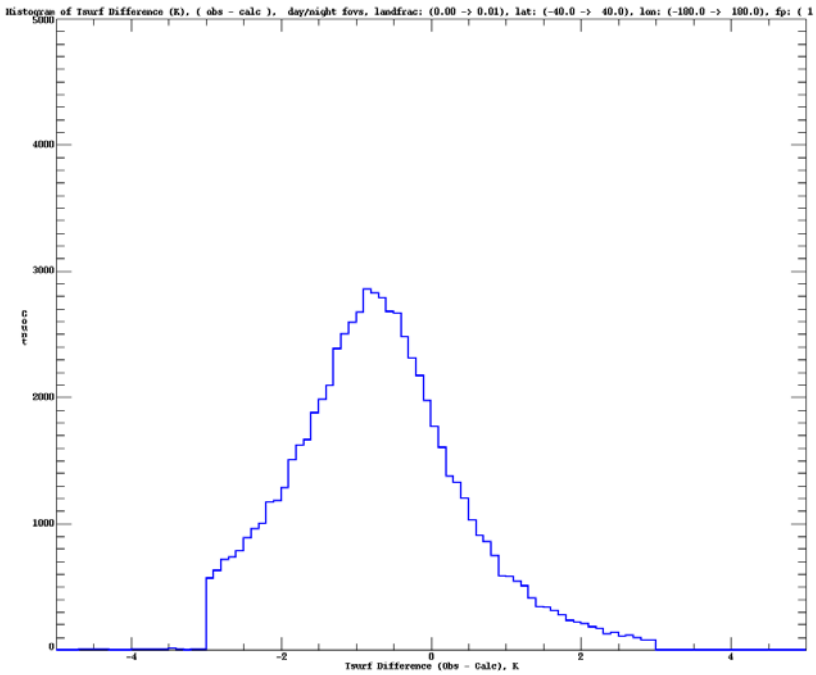

Figure 31. Histogram of the SST differences mapped in Figure 30. The abscissa range is –5 to 5 K. The mean and standard deviation of this distribution are -0.76 ± 0.99 K.

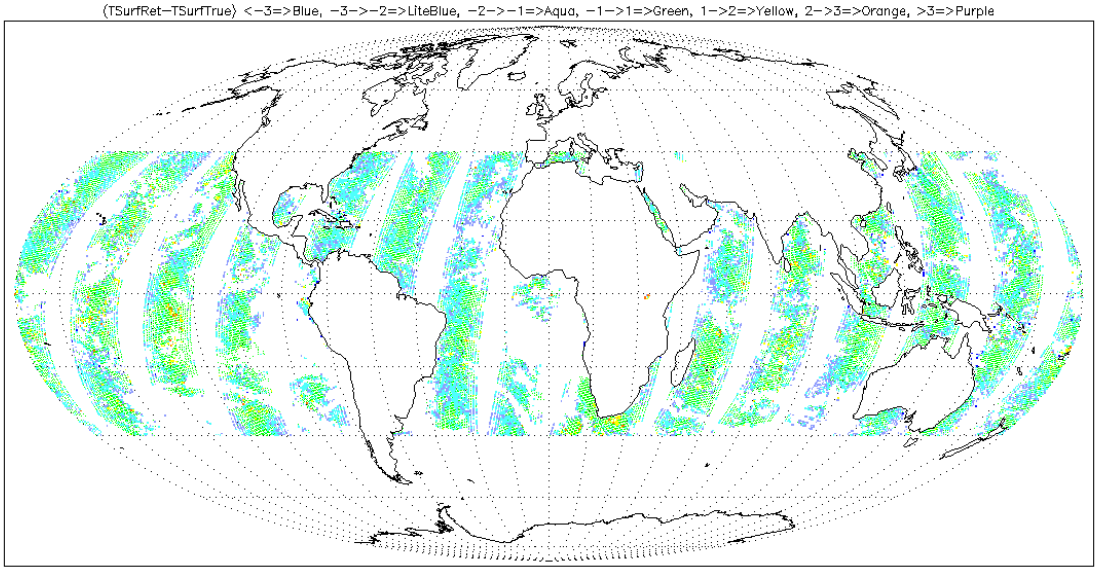

Figure 32. As Figure 30, nighttime only.

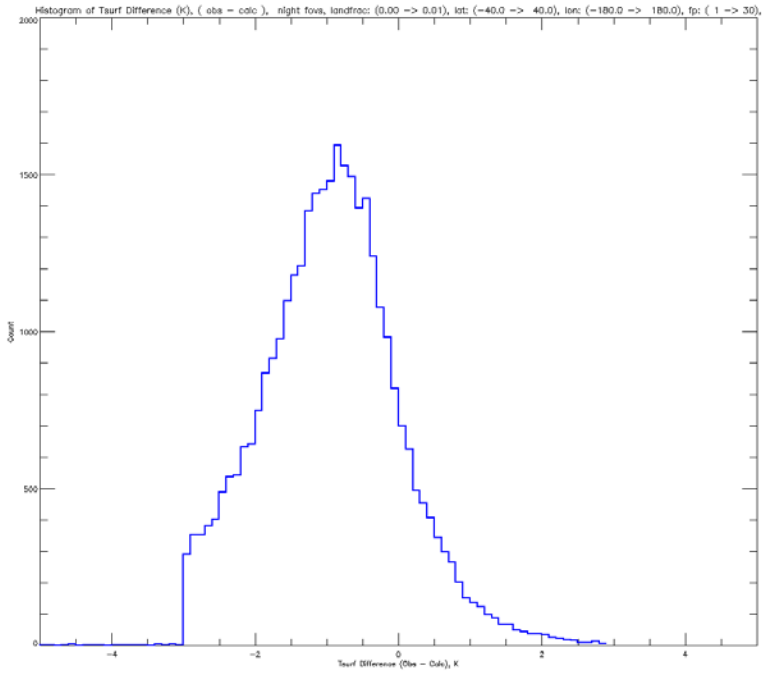

Figure 33. As Figure 31, nighttime only. The mean and standard deviation are –0.94 ± 0.99.

6.4. Provisional Validation of Temperature Profiles

AIRS retrieved temperatures are compared with ECMWF analyses, operational radiosondes, and dedicated radiosondes. The resulting root-mean-square (rms) differences are better than 1 K / km for those retrieval footprints identified as very clear. Errors for other, cloudier profiles are slightly greater than 1 K throughout the lower troposphere, with higher degradation immediately above the surface and around the tropopause.

See Susskind et al. (2003) for retrieval computational error uncertainties in the products discussed below.

6.4.1. Comparison with ECMWF Model Analyses

This section describes comparisons between AIRS temperature retrievals and ECMWF analyses. The comparisons are made by averaging both fields over 1 km thick layers, differencing the averages, then compiling statistics on the differences. Fishbein et al., 2003, describes the method for interpolating the synoptic ECMWF to the location of the AIRS/AMSU/HSB observations.

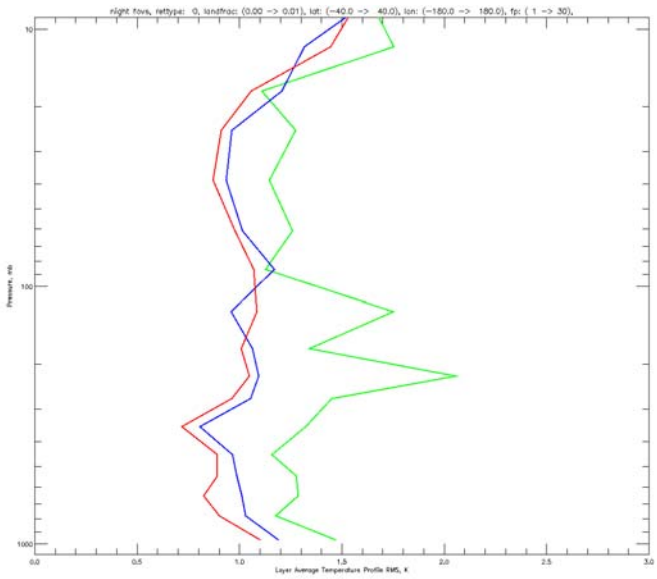

Figure 34. Nighttime only root-mean-square difference over 1 km layers between AIRS retrievals and ECMWF analyses for 6 September 2002. Statistics are for oceans between 40S-40N, where retrieval SST agrees with NCEP forecast to 3.0 K. Green is for the microwave-only retrieval solution, blue is for the regression retrieval solution, and red is the final retrieval solution. X-axis range is 0 to 3 K, and y-axis range is 1100 to 10 mb.

Figure 34 shows the rms difference between AIRS and ECMWF temperatures for 6 September 2002 for oceans between 40 S and 40 N, with retrievals rejected that show disagreement of 3.0 K between AIRS retrieved and NCEP forecast.

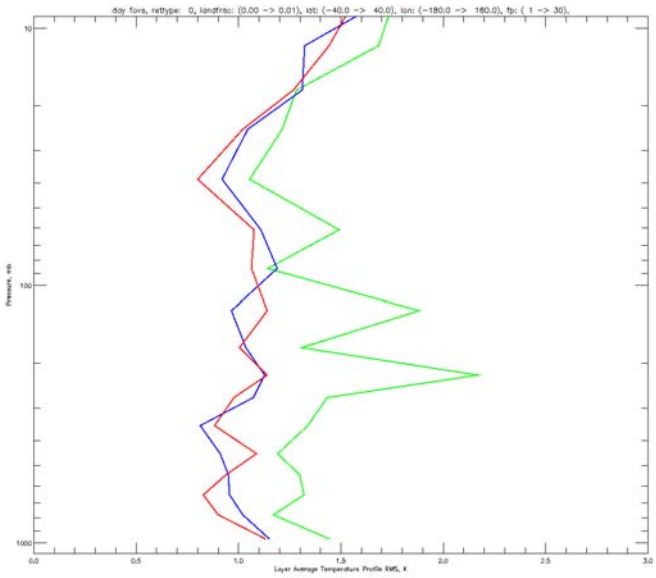

Figure 35. Same as Figure 34 except daytime.

The temperature bias in the retrieval during daytime is shown in Figure 36. The mid-troposphere maximum positive value is roughly twice as large as during nighttime (not shown), suggesting further that convective clouds degrade retrieval performance during daytime. The oscillatory nature of the bias in Figure 36 is a well-recognized aspect of the AIRS and other retrieval systems (see examples in Susskind et al, 2003).

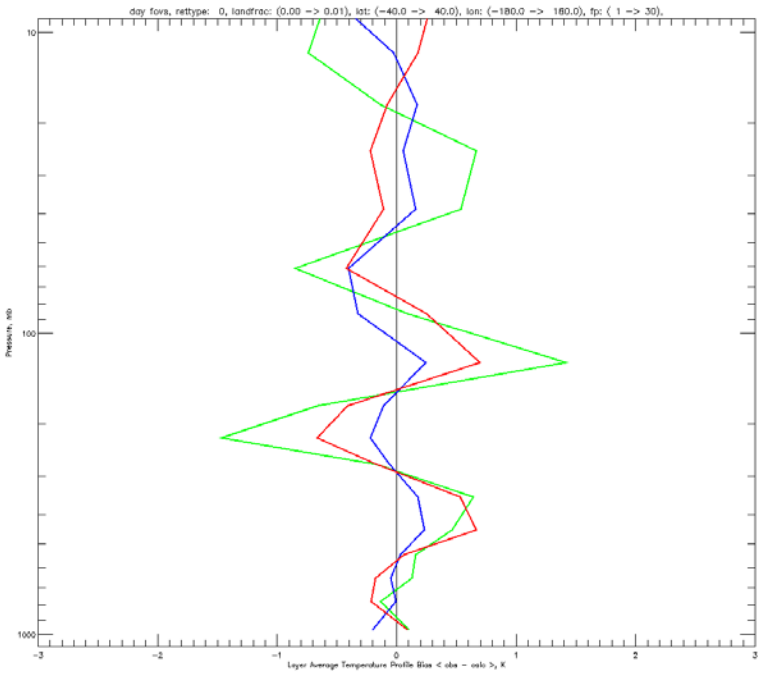

Figure 36. Retrieval bias associated with Figure 35. X-axis range is –3 to 3 K.

6.4.2. Comparison with Dedicated Radiosondes

Figure 37 shows a comparison between AIRS retrieved temperatures and dedicated radiosonde temperature observations at the Chesapeake Light Platform. These sondes were launched during Aqua spacecraft overpasses to minimize spatio-temporal mismatch errors. The higher average difference in Figure 37 compared with Figure 34 and Figure 35 is likely due to the more difficult retrieval conditions in the ocean adjacent to continents.

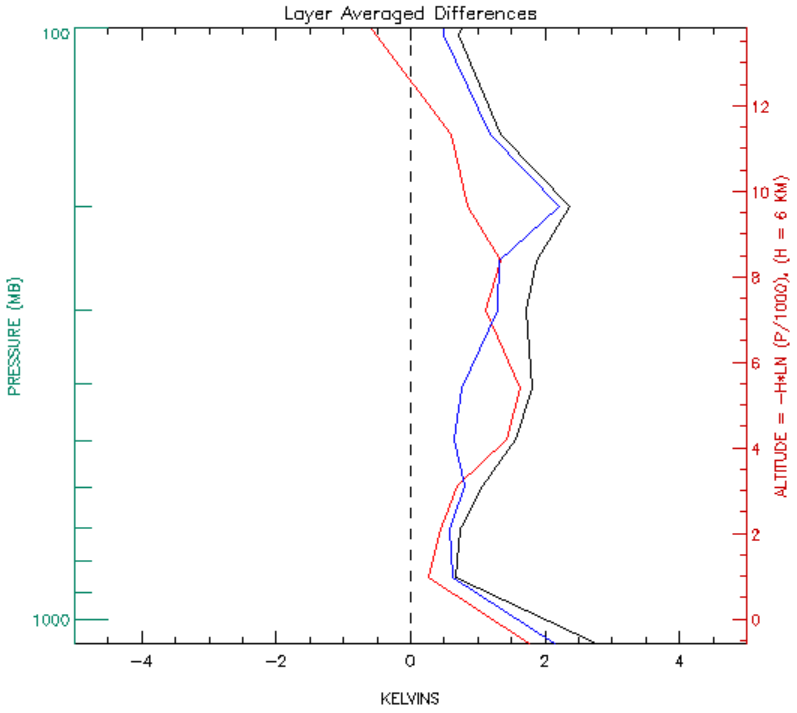

Figure 37. One-kilometer thick layer average temperature difference between AIRS final retrieval and 30 radiosondes launched from Chesapeake Light Platform between 4 September and 5 October 2002. Red curve is bias, blue is standard deviation, and black is rms. Note that color palette is different from previous two figures.

6.5. Beta Validation of Total Water Vapor

Table 8 summarizes the results of validation analyses for total water vapor. The ECMWF and operational sonde values of 14-16% rms are statistically most significant with thousands of comparisons each. The dedicated sondes are of high quality but limited to tens of comparisons per site. The large, negative bias at the ARM Tropical Western Pacific site on Nauru Island is a recognized retrieval problem for very moist atmospheres. Nauru is climatologically the wettest atmosphere on the planet, with total water loading up to 80 mm, compared to 20-60 mm for operational sondes (compare Figure 39 and Figure 40 for relative magnitudes of water vapor loading at Nauru and for operational sondes). Nauru is representative of only a small fraction of the planet.

Data source	Relative Bias, percent	Relative RMS, percent
ECMWF analyses	0.01	16.2
Dedicated sondes*	-0.1, -10.0	10.6, 11.4
Operational sondes (Vaisala RS90 only	2.9	11.5

*Chesapeake Platform and ARM Tropical Western Pacific, respectively.

Table 8. Bias and rms relative differences [(AIRS-In Situ)/AIRS] in total water vapor for three data sources.

6.5.1. Comparison with Model Analyses

The comparison with the ECMWF analysis is restricted to oceans between 40S and 40N, where the retrieval agrees with the NCEP forecast to ±3 K (see Figure 22 for an example of the coverage). The results for the ECMWF analysis are shown in Table 8.

6.5.2. Comparison with Dedicated Radiosondes

Figure 38 shows AIRS retrieved total water vapor versus radiosonde observed total water vapor for the Chesapeake Light Platform, 15 km from the mouth of Chesapeake Bay. The sondes were launched between 1 September and 5 October 2002, and the retrieved water vapor is from the nearest AIRS ocean-only locations within 70 km. Note: this plot is not representative of all water vapor present, but only water within the altitudes of coverage by the balloon.

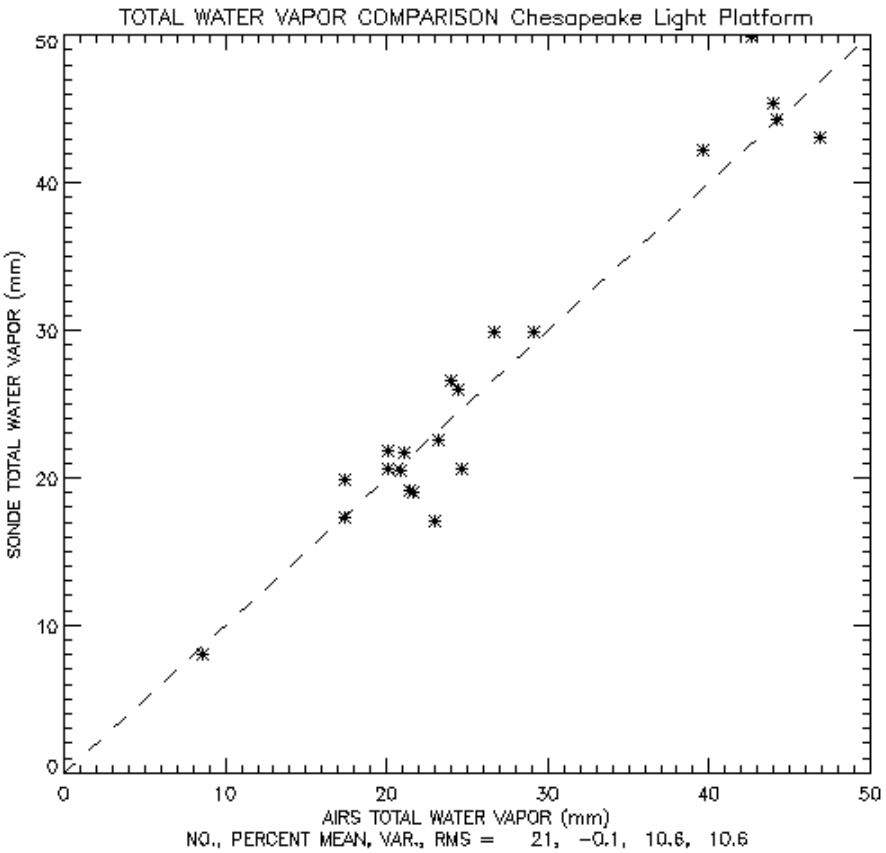

Figure 38. AIRS retrieved total water vapor versus radiosonde observed total water vapor at the Chesapeake Light Platform. Numbers at the bottom of the plot give number of matches, mean variance, and rms differences.

Figure 39 shows is a similar plot but for the ARM Tropical Western Pacific site on Nauru Island (0.34 S, 166.55 E). The sondes were launched between September and December of 2002. The systematically dry AIRS retrieval is associated with an unresolved moist boundary layer in the lowest kilometer of the atmosphere. Understanding and resolving this retrieval bias is an ongoing effort of the AIRS project.

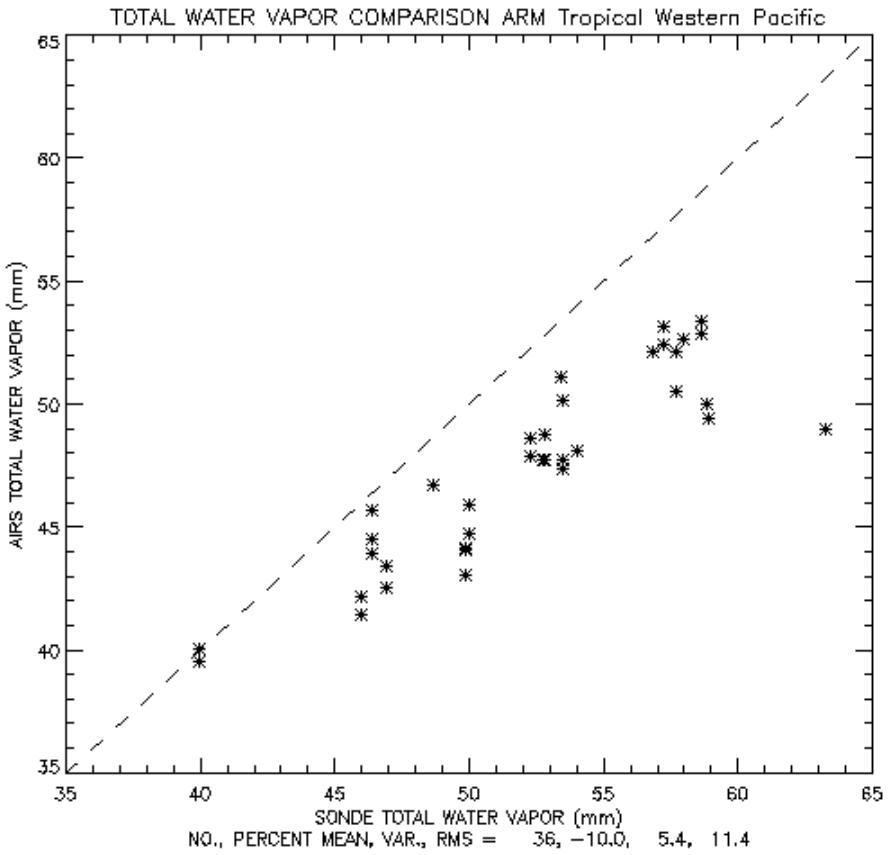

Figure 39. AIRS retrieved total water vapor versus radiosonde observed total water vapor at the at the ARM Tropical Western Pacific site. Numbers at the bottom of the plot give number of matches, mean variance, and rms differences.

6.5.3. Comparison with Operational Radiosondes

AIRS total water vapor compared against matched operational radiosondes for September to December 2002 is shown in Figure 40, with matching criteria of 3 hours and 200 km. This analysis is restricted to Vaisala RS90 sondes, which are the highest quality available.

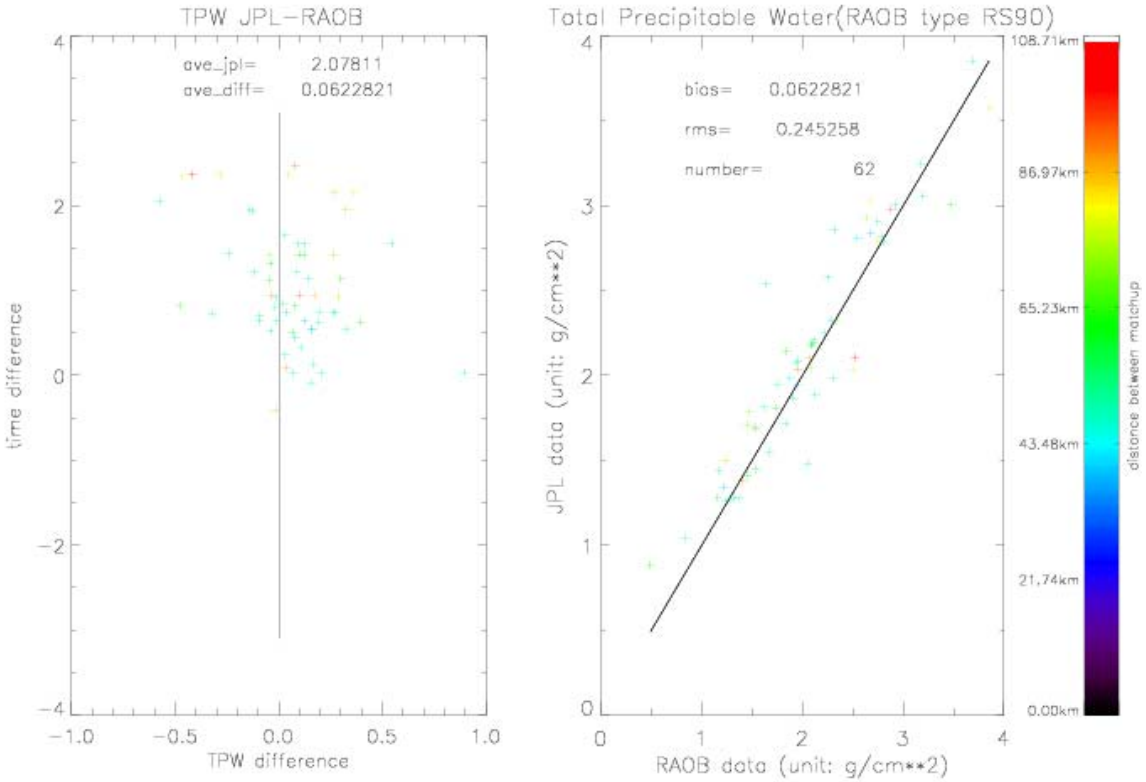

Figure 40. Right panel: Total water vapor in AIRS retrievals versus collocated operational radiosondes, RS90 only. Left panel: coding of differences as a function of space-time match between AIRS and sondes. The average bias of the difference is 2.9%, and its rms is 11.5%.

6.6. Beta Validation of Retrieved Water Vapor Profiles

Water vapor profiles are compared against ECMWF analyses and operational radiosondes. Biases are generally small (except where model fields are suspect), with random errors increasing rapidly with height, from 10-15% near to surface to 30-40% above 500 mb. The retrievals have a known problem near the tropopause, where a non-physical kink in mixing ratio is sometimes retrieved.

6.6.1. Insensitivity to Water Vapor Above Tropopause

AIRS radiances, and the retrievals, are relatively insensitive to water vapor in the stratosphere. The current retrieval algorithm depends heavily upon a climatological water vapor profile above the tropopause. A dry layer near 100 mb is occasionally seen, as in Figure 41, and is an artifact of combining a retrieval in the troposphere with a climatological water vapor profile in the stratosphere.

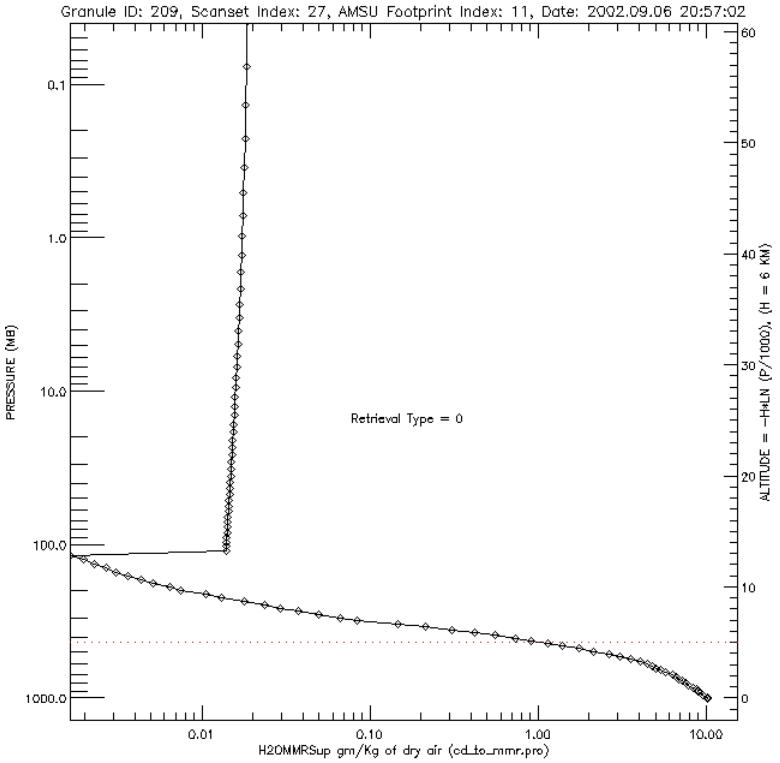

Figure 41. Example of error in fitting water vapor retrieval to climatology in the 100 to 200 mb layer.

6.6.2. Comparison with Model Analyses

The comparison of AIRS water vapor retrievals versus ECMWF model results for combined day and night on 6 September 2002 is show in Table 9. Water vapor retrievals have a small diurnal amplitude in rms errors compared to those for temperature (see Section 6.4.1).

Pressure Layer (mb)	Layer Average Bias (%)	Layer Average RMS (%)
1100 to 700	-1.8	9.8
700 to 500	-1.1	31.2
500 to 350	-12.5	32.5

Table 9. Difference in retrieved water vapor profiles compared with ECMWF analyses, relative to AIRS [(AIRS-sonde)/AIRS in percent] for 6 September 2002, combined day and night.

6.6.3. Comparison with Operational Radiosondes

The comparison of AIRS water vapor retrievals versus operations sondes for combined day and night for the months of September through December 2002 is show in Table 10. The analysis is limited to Vaisala RS90 sondes. Scatterplots of the observation used to generate Table 10 are shown below.

Pressure Layer	Layer Average Bias (%)	Layer Average RMS (%)
1100 to 700 mb	3.6	11.6
700 to 500	0.0	26.5
500 to 350	-3.7	50.5

Table 10. Difference in retrieved water vapor profiles compared with operational radiosondes, relative to AIRS [(AIRS-sonde)/AIRS in percent] for September to December 2002.

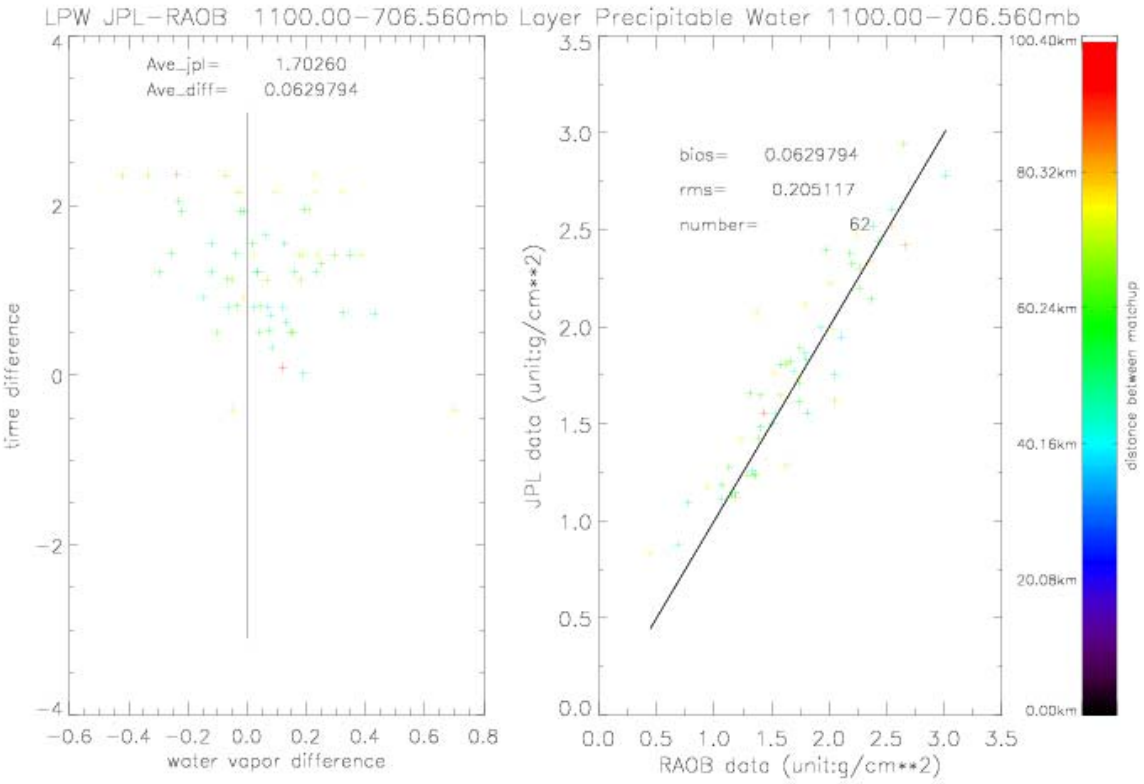

Figure 42. AIRS retrieved total water vapor versus operational RS90 sonde total water vapor in the 1100 to 700 mb layer.

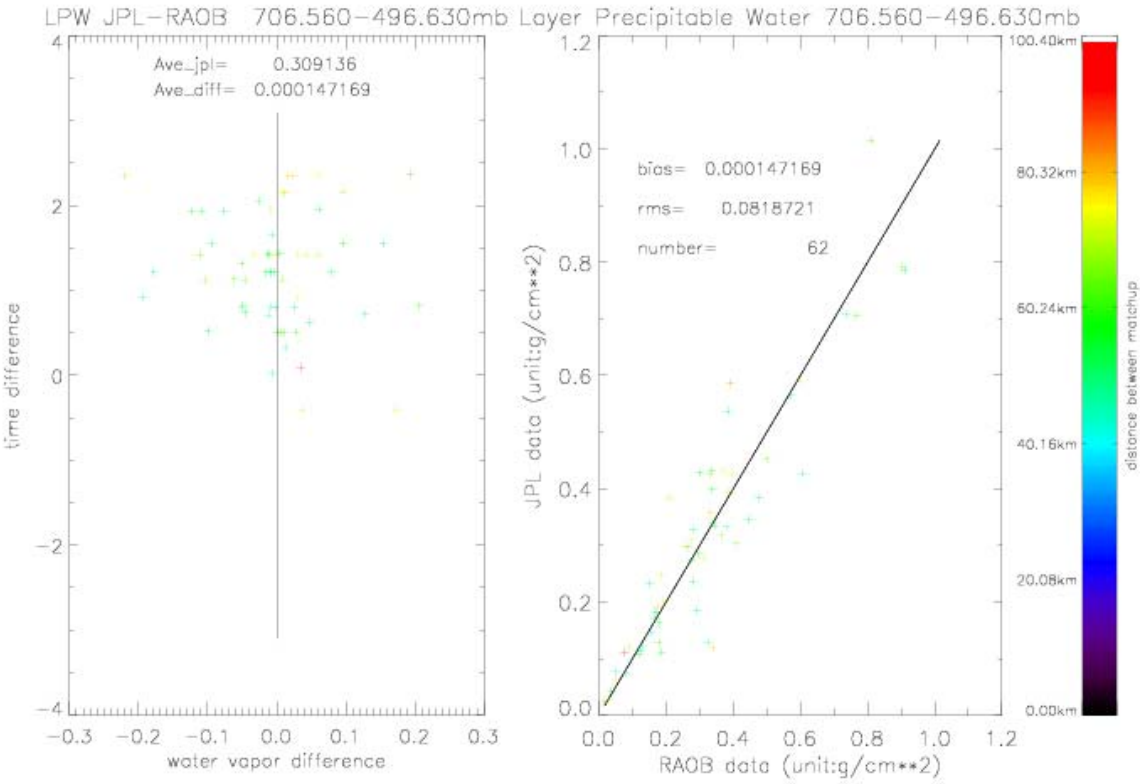

Figure 43. AIRS retrieved total water vapor versus operational RS90 sonde total water vapor in the 700 to 500 mb layer.

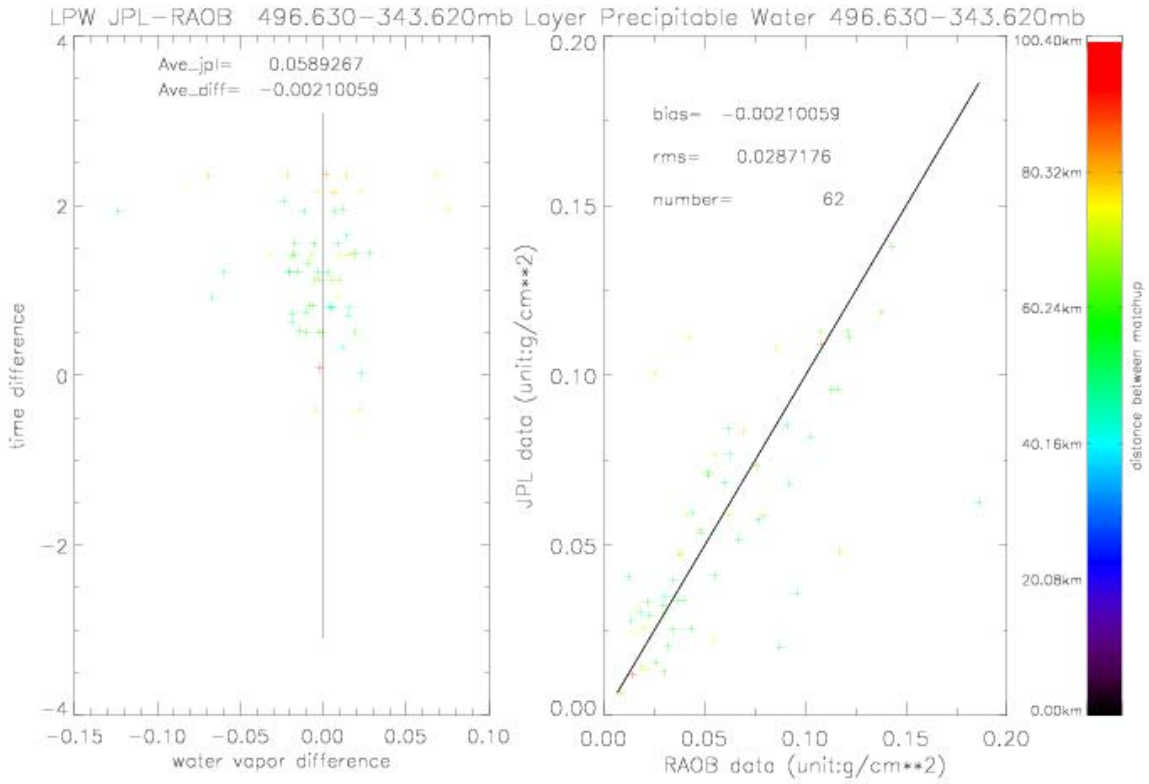

Figure 44. AIRS retrieved total water vapor versus operational RS90 sonde total water vapor in the 500 to 350 mb layer.

7. Appendix I: H. Revercomb AIRS Level 1B Evaluation / Validation Material

This section describes the complete set of AIRS radiance validation activities by AIRS Science Team Member H. Revercomb and colleagues D. Tobin, R. Frey and others of the University of Wisconsin at Madison.

Individual presentations named in the section below are posted online at http://airs3.ssec.wisc.edu/~airs/level1Bmaterial/supporting_material/aaasbe.ppt and http://airs3.ssec.wisc.edu/~airs/level1Bmaterial/other_references/

This report outlines material prepared under the AIRS Science Team Member contract of H. E. Revercomb for inclusion in the AIRS Project Level 1B Validation report.

Revercomb activities related to AIRS Level 1B evaluation / validation include:
1. Early broadband radiance comparisons to GOES-8, 10, and GMS
2. Noise characterization using Earth scene data
3. Aqua radiance intercomparison between AIRS, MODIS, and CERES
4. Cloud Detection
5. Radiance spectra comparisons using calculations based on global radiosondes and ARM site best estimate profiles
6. Analysis of aircraft based infrared observations (S-HIS, NAST-I) for radiance validation
7. Others miscellaneous efforts: a) global IR quicklooks with Aqua and Terra orbit track overlays, b) example effects of C_{ij} illustrated with Hurricane Isadore, c) polar observed/calculated spectra

Following are brief overviews of these activities and some conclusions, with the majority of material included as appendices. The appendices consist of collections of material related to a specific topic, drawing from the AIRS science team meetings, net-meetings, and other relevant meetings and scientific conferences. We anticipate that this material will be used at a later date as input for the comprehensive AIRS Team's Level 1B report. Supporting material and references denoted with a "✣" are provided as part of this report.

1. Early broadband radiance comparisons to GOES-8, 10, and GMS

Early comparisons of AIRS and GOES imager radiances were compared as a rough check on the AIRS radiometric calibration. This is performed using AIRS data collected at the GOES data collected at the GOES sub-satellite point (at the equator) to reduce effects due to mismatched view angles. The comparison technique includes spectral convolution of the AIRS spectra with the GOES spectral response functions, and spatial degradation of both sensors to a common scale. Variability of the GOES radiances within the AIRS FOVs and a basic cloud mask is used to screen the data used in the comparisons. We find very acceptable agreement between AIRS and GOES for all cases

and spectral channels studied. This effort has been absorbed into a larger inter-calibration project conducted by other SSEC personnel.

Supporting Material:

- material presented at various AIRS meetings and net-meetings
  Filename: goes.ppt

Other references:

- Gunshor, M. M., D. Tobin, T. J. Schmit, and W. P. Menzel, 2003: First satellite intercalibration comparing high spectral resolution AIRS with operational geostationary imagers. 12th Conference on Satellite Meteorology and Oceaongraphy, Longbeach, CA, 9-13 February 2003 (preprints). Boston, MA, American Meteorological Society.
  Filename: Intercal_AMSsatcon12_2003_extabs_2columns.doc

2. Noise characterization using Earth scene data

The AIRS noise has been characterized using a Principle Component Analysis (PCA) technique applied to
Earth scene spectra. NeDT values from random detector noise derived from the PCA technique agree well with values reported in both the channel properties files and with values provided in the Level 1 B granule files. Also, the spatially/temporally correlated signatures associated with "popping" noise was demonstrated with geographic maps of brightness temperature differences of adjacent AIRS channels. PCA techniques were further used to perform a quantitative study of the popping noise observed in Earth scene data. Most importantly, the PCA technique was demonstrated to work in a noise filtering mode to remove both random and popping noise from the AIRS spectra.

Supporting material :

- material presented at various AIRS meetings and net-meetings.
  Filename: noise.ppt

Other references:

- Tobin, D. C., H. E. Revercomb, S. A. Ackerman, P. Antonelli, M. Gunshor, R. O. Knuteson, C. Moeller, Characterization of Atmospheric Infrared Sounder (AIRS) Earth Scene Radiances, in *Fourier Transform Spectroscopy*, OSA Technical Digest (Optical Society of America, Washington DC, 2003), Quebec City, 3-6 February 2003.
  Filenames: tobin_quebec_2003.ppt, tobin_quebec_2003_abstract.doc

- Revercomb et al., "Applications of high spectral resolution FTIR observations demonstrated by the radiometrically accurate ground-based AERI and the Scanning HIS aircraft instruments". SPIE 3rd International Asia-Pacific Symposium on Remote Sensing of the Atmosphere, Ocean, Environment, and Space Hangzhou, China, 23-29 October 2002.

3. Aqua radiance intercomparison between AIRS, MODIS, and CERES

Intercomparison of AIRS and MODIS radiances is performed by convolving AIRS spectra with the MODIS spectral response functions, and reducing the MODIS data to AIRS spatial resolution. Variability of the MODIS data collocated with the AIRS FOVs and a basic cloud mask is used to screen data which is used in the comparisons. In general we find very good agreement between AIRS and MODIS radiances. For the longwave MODIS bands, however, we find a small radiance bias between MODIS and AIRS which increases from near zero mean for MODIS band 32 at ~12.0 microns to just over 1K for MODIS Band 36 at ~14.2 microns, with MODIS being warmer than AIRS. For the limited number of cases studies so far, this bias does appear to have a signal dependence, with essentially no bias observed for very cold scenes over Antarctica. A possible explanation is small uncertainties in knowledge of the MODIS spectral response functions.

Supporting material :

- material presented at various AIRS meetings and net-meetings.
  Filename: modis.ppt

Other references:

- Tobin, D. C., H. E. Revercomb, S. A. Ackerman, P. Antonelli, M. Gunshor, R. O. Knuteson, C. Moeller, Characterization of Atmospheric Infrared Sounder (AIRS) Earth Scene Radiances, in *Fourier Transform Spectroscopy*, OSA Technical Digest (Optical Society of America, Washington DC, 2003), Quebec City, 3-6 February 2003.
  Filenames: tobin_quebec_2003.ppt, tobin_quebec_2003_abstract.doc

4. Cloud Detection

Detection of clouds in the AIRS field of view is important for radiance bias and forward model evaluation using observed and calculated spectra. For this effort, we have developed two basic cloud detection algorithms. One uses spectral and spatial tests based on AIRS data alone. The other collocates the MODIS and AIRS data to produce a MODIS cloud mask product which is relevant to the AIRS fields of view. This is referred to as the "condensedMODIS" cloud flag. For specific "focus days", we have provided these products for the entire globe/day for evaluation and have also used them for our clear sky observed/calculated studies. In general, the MODIS information greatly improves the ability to detect clouds within the AIRS fields of view. To identify severe clear cases for night-time ocean, combined MODIS/AIRS cloud detection techniques are not always adequate. Efforts to determine the optimal use of the high spectral (AIRS) and high spatial (MODIS) resolution information to produce a combined AIRS/MODIS cloud mask are on-going.

Supporting material :

- material presented at various AIRS meetings and net-meetings.
  Filename: clouds.ppt

Other references:

- Frey, R. A., D. C. Tobin, S. A. Ackerman, Cloud Detection with MODIS and AIRS, in *Optical Remote Sensing*, OSA Technical Digest (Optical Society of America, Washington DC, 2003), Quebec City, 3-6 February 2003.

5. Radiance spectra comparisons using calculations based on global radiosondes and ARM site best estimate profiles

The high accuracy retrieval goals of AIRS (1K rms in 1km layers below 100mbar for temperature, 10% rms in 2km layers below 100 mbar for water vapor, 0.5K for surface skin temperature), combined with the large temporal and spatial variability of the atmosphere and certain difficulties in making accurate measurements of the atmospheric state, necessitates careful and detailed validation using well characterized ground based sites. As part of on-going AIRS Science Team efforts and a collaborative effort between NASA and ARM, data from various ARM and other observations are used to create best estimates of the atmospheric state at the Aqua overpass times. This draws upon previous and on-going studies and careful characterization and knowledge of the ARM data streams. For some overpasses which meet specific view angle and weather related requirements, dedicated radiosondes are launched just before (~45 minutes) and at the overpass time. Estimates of the spectral surface emissivity and local skin temperatures are also constructed. These products and auxiliary images/plots are made available on the web for each overpass.

These profiles and collocated clear sky AIRS data are being used to study observed minus calculated AIRS spectra, aimed at evaluation of the AIRS forward model, AIRS radiances, and the input atmospheric state. We are also performing similar but limited efforts using global radiosondes as input to the calculations. These investigations are done in collaboration with the UMBC group. The ARM best estimate products (and products from similar ARM-like sites) are proving to be invaluable for this effort. Bias estimates from the ARM site are compared to estimates derived from global ocean nighttime radiosondes and using ECMWF analysis fields as input to the forward model. Differences in both the mean and variability of the results, particularly regarding spectral channels sensitive to boundary layer and upper level water vapor, are attributed to better temporal / spatial collocation and accuracy of the ARM site profiles. The early observed minus calculated results demonstrate that the high quality ARM atmospheric state best estimate profiles are necessary for the ultimate validation of AIRS and that global statistical data is not adequate alone.

Supporting material :

- material presented at various AIRS meetings and net-meetings relating to observed minus calculated studies.
  Filename: obscalc.ppt
- material presented at various AIRS meetings and net-meetings relating to development and production of the AIRS ARM Atmospheric State Best Estimates.

Filename: aaasbe.ppt

Other references:

- Tobin, D. C., H. E. Revercomb, D. D. Turner, *Radiosondes: the ARM and AIRS Perspectives*, presented at the Workshop to Improve the Usefulness of Operational Radiosonde Data, 11-13 March 2003, Asheville, NC. *Filename: tobin_sonde_wkshp_march2003.ppt*
- Strow, L. L., Hannon, S. E., S. DeSouza Machado, H. Motteler, Validation of the AIRS radiative transfer algorithm, in *Optical Remote Sensing*, OSA Technical Digest (Optical Society of America, Washington DC, 2003), Quebec City, 3-6 February 2003.
- Tobin, D. C., H. E. Revercomb, W. F. Feltz, R. O. Knuteson, D. D. Turner, B. M. Lesht, L. L. Strow, E. J. Fetzer, ARM Site Atmospheric State Best Estimates for AIRS Validation, in Proceedings of the Thirteenth ARM Science Team Meeting, Broomfield, CO, 31 March – 4 April 2003. *Filename: arm_stm_2003.aaasbe.extabstract.doc*
- Knuteson, R. O., R. G. Dedecker, W. F. Feltz, B. J. Osborne, H. E. Revercomb, H. E., and D. C. Tobin, Infrared Land Surface Emissivity in the Vicinity of the ARM SGP Central Facility, in Proceedings of the Thirteenth ARM Science Team Meeting, Broomfield, CO, 31 March – 4 April 2003.
- Revercomb, H. E., D. C. Tobin, D. D. Turner, et al., The Atmospheric Radiation Measurement Program's Water Vapor Intensive Observation Periods: Overview, Accomplishments, and Future Challenges, *BAMS*, **84**, 217-236, 2003.
- Tobin, D. C, H. E. Revercomb, D. D. Turner, Overview of the AMR/FIRE Water Vapor Experiment (AFWEX), in Proceedings of the Twelfth ARM Science Team Meeting, St. Petersburg, FL, 8-12 March 2002.
- Turner, D. D., B. M. Lesht, S. A. Clough, J. C. Liljegren, H. E. Revercomb, D. C. Tobin, Dry Bias and Variability in Vaisala Radiosondes: The ARM Experience, *J. Atmospheric and Oceanic Technology*, **20**, 117-132, 2003.

6. Analysis of aircraft based infrared observations (S-HIS, NAST-I) for radiance validation

A particularly critical assessment of AIRS spectral radiances involves comparison of the AIRS radiances with collocated high spectral resolution radiances measured with the high altitude aircraft-based Scanning-HIS. Two cases have been analyzed in detail to date: a clear sky case over the ARM SGP site on 16 November 2002 as part of the ARM UAV campaign, and a clear sky case over the Gulf of Mexico as part of the Texas-2002 Aqua Level 1B validation campaign. Differences in sensor spectral resolution and sampling, spatial resolution and sampling, and platform altitudes are accounted for in the analysis technique. For both cases, in general, we find excellent agreement (of order 0.1K) between the AIRS and Scanning-HIS observed spectra. One issue, related to the spectral knowledge of AIRS detector module 5, was identified with this analysis.

These results clearly demonstrate the importance of aircraft intercomparison for on-going validation of EOS observations needed for climate studies.

Supporting material :

- material presented at various AIRS meetings and net-meetings.
  Filename: aircraft.ppt

Other references:

- Revercomb, H.E., V.P. Walden, D. C. Tobin, J. Anderson, F.A. Best, N.C. Ciganovich, R.G. Dedecker, T. Dirkx, S.C. Ellington, R.K. Garcia, R. Herbsleb, H.B. Howell, R.O. Knuteson, D. LaPorte, D. McRae, and M. Werner, Recent Results from Two New Aircraft-based Instruments: the Scanning High-resolution Interferometer Sounder (S-HIS) and the NPOESS Atmospheric Sounder Testbed-Interferometer (NAST-I), Eighth International Workshop on Atmospheric Science from Space using Fourier Transform Spectrometry (ASSFTS8), Toulouse, France, 16-18 November, 1998.
- Revercomb, H. E., D. C. Tobin, R. O. Knuteson, F. A. Best, W. L. Smith, P. van Delst, D. D. LaPorte, S. D. Ellingson, M. W. Werner, R. G. Dedecker, R. K. Garcia, N. Ciganovich, H. B. Howell, Atmospheric Infrared Sounder (AIRS) validation with Scanning-HIS, in *Fourier Transform Spectroscopy*, OSA Technical Digest (Optical Society of America, Washington DC, 2003), Quebec City, 3-6 February 2003.
  Filename: revercomb_quebec_2003-f.ppt
- Tobin, D. C., H. E. Revercomb, S. A. Ackerman, P. Antonelli, M. Gunshor, R. O. Knuteson, C. Moeller, Characterization of Atmospheric Infrared Sounder (AIRS) Earth Scene Radiances, in *Fourier Transform Spectroscopy*, OSA Technical Digest (Optical Society of America, Washington DC, 2003), Quebec City, 3-6 February 2003.
  Filenames: tobin_quebec_2003.ppt, tobin_quebec_2003_abstract.doc

7. Other miscellaneous efforts

Other recent efforts related to Level 1B characterization of possible interest are:

- global IR quicklooks with Aqua and Terra orbit track overlays
- example effects of Cij illustrated with Hurricane Isadore, and
- polar observed/calculated spectra

Supporting material:

- *Filename: misc.ppt*

8. Appendix II: Beta Validation of Total Ozone

Dr. Michael Newchurch of University of Alabama at Huntsville is leading the validation of AIRS ozone, with JPL co-investigators Drs. Michael Gunson and Fredrick Irion. Initial comparisons of AIRS ozone retrievals have been with Earth Probe-Total Ozone Mapping Spectrometer (EP-TOMS) total ozone column. Comparisons shown use the same filtering criteria as for other retrieved quantities discussed in this report (full infrared retrieval, 40°S – 40°N latitude, land fraction < 0.01, and agreement with NCEP SST analyses to 3.0 K), Figure 45 below illustrates daytime ozone column retrievals for the September 6, 2002 "golden day."

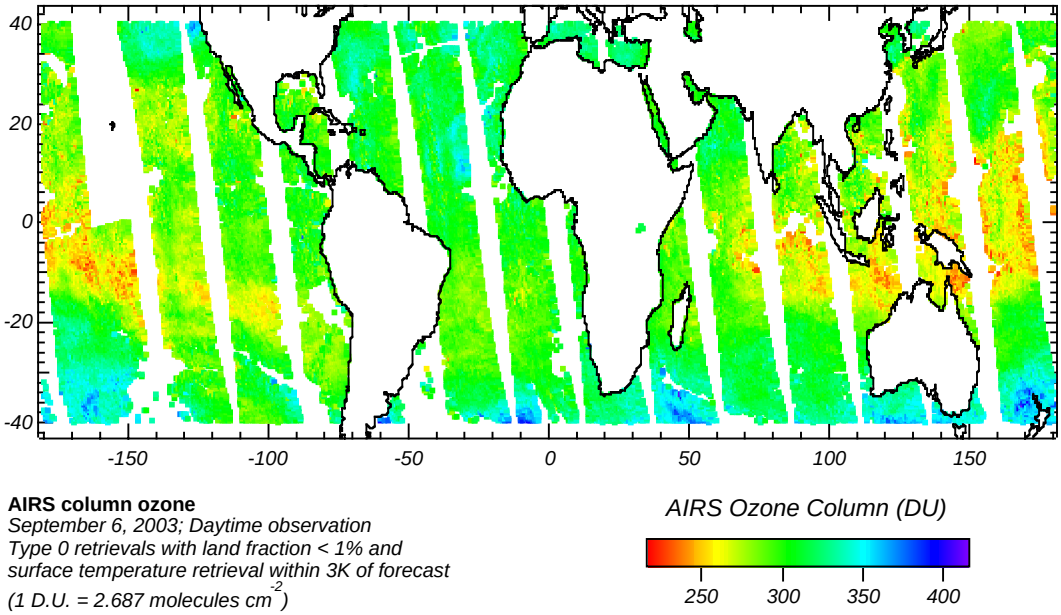

Figure 45. AIRS column amounts over water for September 6, 2002.

Figure 46 compares these AIRS ozone columns with gridded EP-TOMS data (from the GSFC website at http://jwocky.gsfc.nasa.gov/eptoms/ep.html.) EP-TOMS has a sun-synchronous orbit with an ascending equator crossing time of 11:16 AM (compared with 1:30 PM for Aqua). AIRS total column ozone is higher than TOMS by an average of 4.4 ± 5.3%. A notable increase of AIRS column ozone compared with TOMS can be seen off the coast of northwest Africa, possibly related to dust being blown off the continent. Figure 47 shows this AIRS/TOMS relative difference increases slightly in the presence of high clouds.

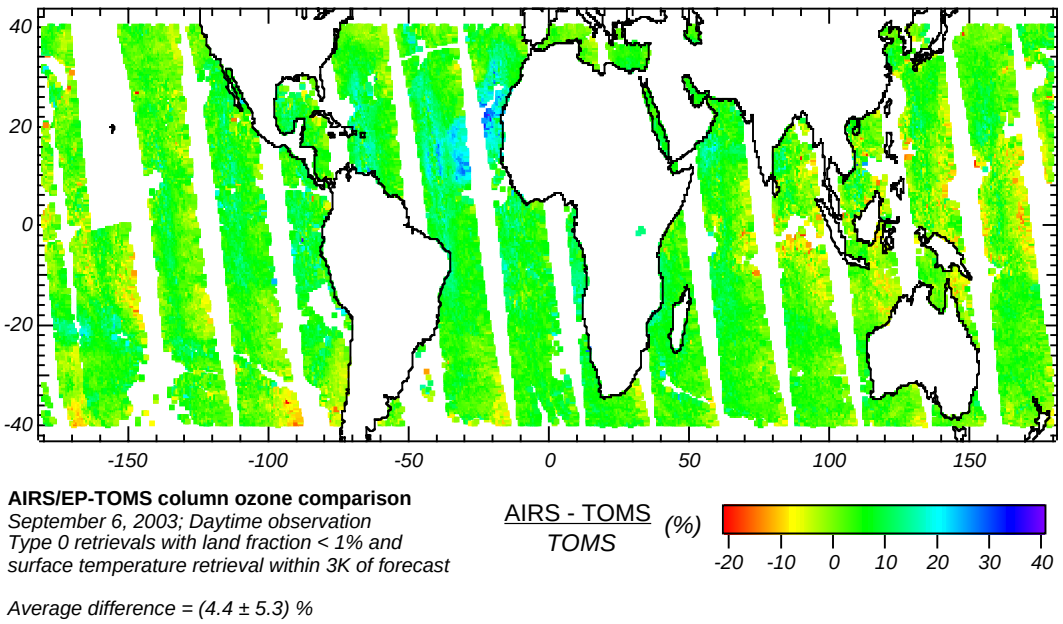

Figure 46. Relative difference between AIRS and TOMS total ozone column for September 6, 2002.

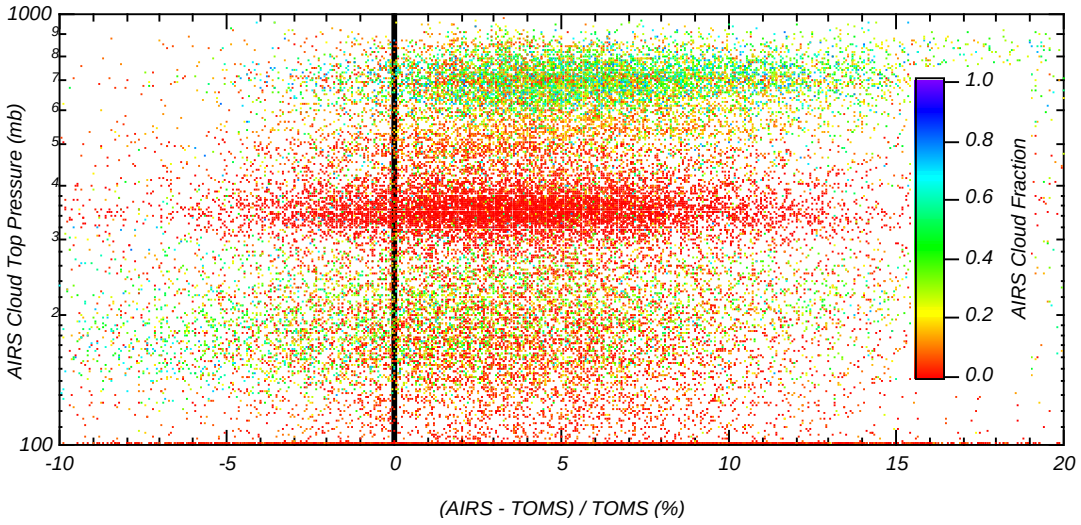

Figure 47. Relative difference between AIRS and TOMS as a function of retrieved cloud-top height.

9. Appendix III: Pressure Levels Used for Vertical Averages

The following tables give the layers used for averaging of temperature and water vapor in Chapter 6.

Temp Avg Layer Number	Standard Pressures (mb)	Layer Thickness (km)*	Support Product Levels (mb)	Support Product Level Index
1	850 – 1100	1.8 (1.24 above 100 mb)	852.788025 - 1100	91 - 100
2	700 – 850	1.35	706.565430 - 852.788025	85 - 91
3	600 – 700	1.07	596.306213 - 706.565430	80 - 85
4	500 – 600	1.27	496.629791 - 596.306213	75 - 80
5	400 – 500	1.56	407.473785 - 596.306213	70 - 75
6	300 – 400	2.01	300.000000 - 407.473785	63 - 70
7	250 – 300	1.27	247.408493 - 300.000000	59 - 63
8	200 – 250	1.56	200.988693 - 247.408493	55 - 59
9	150 – 200	2.01	151.266403 - 200.988693	50 - 55
10	100 – 150	2.84	103.017197 - 151.266403	44 - 50
11	70 – 100	2.50	71.539803 - 103.017197	39 - 44
12	50 – 70	2.36	51.527802 - 71.539803	35 - 39
13	30 – 50	3.58	29.121000 - 51.527802	29 - 35
14	20 – 30	2.34	20.922400 - 29.121000	26 - 29
15	15 – 20	2.01	14.455900 - 20.922400	23 - 26
16	10 – 15	2.84	9.511900 - 14.455900	20 - 23
17	7 – 10	2.50	6.956700 - 9.511900	18 - 20
18	3 – 7	5.93	2.700900 - 6.956700	13 - 18
19	1.5 – 3	4.85	1.687200 - 2.700900	11 - 13
20	.5 - 1.5	7.69	0.506400 - 1.687200	7 - 11
21	.5 to space	thick		7 - 1

*Thickness = $-H \ln(p_i / p_{i-1})$, H = 7 km

Table 11. Layers used in calculating average temperature statistics.

Humidity Averaging Layer number	Standard Pressures (mb)	Layer Thickness (km)	Support Product Level index
1	700 – 1100	3.16 (2.50 above 100 mb)	85 - 100
2	500 – 700	2.34	75 - 85
3	350* – 500 becomes 343.618 – 496.63	2.50	66 - 85
4	200 – 350*	2.36	55 - 66
5	150 - 200	2.01	50 - 55
6	100 – 150	2.84	44 - 50
	30 – 100	8.44	29 - 44
	10 — 30	7.19	20 - 29
7	10 to space	Real thick	1 - 20

* Not an AIRS standard level.

Table 12. Layers used in calculating average humidity statistics.

10. List of Acronyms

ADFM	AIRS Design File Memorandum
AIRS	Atmospheric Infrared Sounder
AMSU	Advanced Microwave Sounding Unit
ARM	Atmospheric Radiation Measuring
ECMWF	European Center for Mediumrange Weather Forecasting
GTS	Global Telecommunications System
HIS	High-resolution Infrared Sounder
HSB	Humidity Sounder for Brazil
IEEE	Institute of Electrical and Electrons Engineers
M-AERI	Marine-Atmospheric Emitted Radiance Interferometer
NCEP	National Center for Environmental Prediction
NOAA	National Oceanic and Atmospheric Administration
PGE	Product Generation Executable
RTG	Real Time Global
SST	Sea Surface Temperature or Surface Skin Temperature
TOA	Top of Atmosphere
TOMS	Total Ozone Mapping Spectrometer
UCSB	University of California at Santa Barbara

11. References

Aumann, H. H., M. T. Chahine and D. Barron, "Sea Surface Temperature Measurements with AIRS: RTG.SST comparison", SPIE 48th International Symposium on Optical Science and Technology, San Diego, CA, 3 August 2003.

Aumann, H. H., M. T. Chahine, C. Gautier, E. Kalnay, L. M. McMilllin, H. Revercomb, P. W. Rosenkranz, W. L. Smith, D. H. Staelin, L. L. Strow and J. Susskind, "AIRS/AMSU/HSB on the Aqua mission: design, science objectives, data products and processing", *IEEE Trans. Geosci. Remote Sensing*, vol. 41, pp. 253-264, Feb. 2003a.

Fetzer, E., L. McMillin, D. Tobin, M. Gunson, H. H. Aumann, W. W. McMillan, D. Hagan, M. Hofstadter, J. Yoe, D. Whiteman, R. Bennartz, J. Barnes, H. Vömel, V. Walden, M. Newchurch, P. Minnett, R. Atlas, F. Schmidlin, E. T. Olsen, M. D. Goldberg, Sisong Zhou, HanJung Ding and H. Revercomb, "AIRS/AMSU/HSB validation", *IEEE Trans. Geosci. Remote Sensing*, vol. 41, pp. 418-431, Feb. 2003.

Fishbein, E. F., C. B. Farmer, S. L. Granger, D. T. Gregorich, M. R. Gunson, S. E. Hannon, M. D. Hofstadter, S.-Y. Lee, S. Leroy, and L. L. Strow, "Formulation and validation of simulated data for the atmospheric infrared sounder (AIRS)", *IEEE Trans. Geosci. Remote Sensing*, vol. 41, pp. 314-329, Feb. 2003

Gaiser, S. L., H. H. Aumann, L. L. Strow, S. E. Hannon, and M. Weiler, "In-flight spectral calibration of the atmospheric infrared sounder (AIRS)", *IEEE Trans. Geosci. Remote Sensing*, vol. 41, pp. 287-297, Feb. 2003

Gautier, C., Y. Shiren, L. L. and M. D. Hofstadter, "AIRS vis/near IR instrument", *IEEE Trans. Geosci. Remote Sensing*, vol. 41, pp. 330-342, Feb. 2003.

Hagan, D., AIRS Design File Memorandum #637 March 14, 2003.

Hagan, D. and P. Minnett, "AIRS radiance validation over ocean from sea surface temperature measurements", *IEEE Transactions on Geosciences and Remote Sensing*, pp 432-441, 41, 2003.

Kahn, B. H., A. Eldering, S. A. Clough, E. J. Fetzer, E. Fishbein, M. R. Gunson, S.-Y. Lee, P. F. Lester and V. J. Realmuto, "Near micron-sized cirrus cloud particles in high-resolution infrared spectra: an orthographic case study", *Geophys. Res. Letters*, vol. 30, no. 8, p. 1441, 2003.

Lambrigtsen, B. H., and R. V. Calheiros, "The humidity sounder for Brazil--an international partnership", *IEEE Trans. Geosci. and Remote Sensing, 41*, 2, pp 352-361, 2003.

Masuda, K., T. Takashima and T. Takayama, "Emissivity of pure and sea waters for the model sea surface in the infrared window region," *Remote Sens. Environ.*, vol 24, pp 313-329, 1988.

Pagano, T. S., H. H. Aumann, D. E. Hagan and K. Overoye, "In-flight spectral calibration of the atmospheric infrared sounder (AIRS)", *IEEE Trans. Geosci. Rem. Sens.*, 41, 265-273, 2003.

Rosenkranz, P. W., Rapid radiative transfer model for AMSU/HSB channels, *IEEE Trans. Geosci. Rem. Sens.*, 41, 362-368, 2003.

Strow, L. L.., S. Hannon, S. DeSouza Machado, H. Motteler, and D. T. Gregorich, ”An overview of the AIRS radiative transfer model”, *IEEE Trans. Geosci. Remote Sensing*, vol. 41, pp. 274-286, Feb. 2003.

Strow, L. L.., S. Hannon, M. Weiler, K. Overoye S. L. Gaiser and H. H. Aumann, ”Prelaunch spectral calibration of the Atmospheric Infrared Sounder”, *IEEE Trans. Geosci. Remote Sensing*, vol. 41, pp. 303-313, Feb. 2003.

Susskind, J., C. Barnet and J. Blaisdell, “Retrieval of atmospheric and surface parameters from AIRS/AMSU/HSB in the presence of clouds”, *IEEE Trans. Geosci. Remote Sensing*, vol. 41, pp. 390-409, Feb. 2003.